Miniaturized Charpy Specimens for the Indirect Verification of Small-Scale Charpy Machines: Initial Qualification Phase

Enrico Lucon

NIST

National Institute of Standards and Technology

U.S. Department of Commerce

Miniaturized Charpy Specimens for the Indirect Verification of Small-Scale Charpy Machines: Initial Qualification Phase

Enrico Lucon

Materials Reliability Division
National Institute of Standards and Technology
325 Broadway
Boulder, CO 80305

March 2012

Abstract

Small specimen test techniques become ever more popular as the need increases to characterize mechanical properties by use of the smallest possible amount of material, due to various restrictions on material availability, irradiation, testing space, and other factors.

NIST is currently developing reference miniaturized Charpy V-notch (MCVN) specimens for the indirect verification of small-scale impact testing machines. The same materials used for NIST standard verification specimens are being evaluated at three energy levels (low, high and super-high). Two specimen types are being investigated, denominated KLST (from the German *Kleinstprobe*, or "small specimen") and RHS (reduced half-size).

Several instrumented impact tests on miniaturized KLST and RHS specimens of low, high and super-high energy have been performed and analyzed. The variability of MCVN data has been compared to that of full-size Charpy data from the same lot of test specimens.

Although this can be considered just the preliminary phase of this project, the results indicate that MCVN verification specimens can be used for the indirect verification of small-scale instrumented impact testers, both in terms of absorbed energy and maximum force.

Additional aspects have also been investigated, such as the influence of shear lip symmetry and specimen fracture on absorbed energy and the correlation between miniaturized and full-size Charpy data.

Keywords

Indirect verification; KLST; MCVN; miniaturized Charpy specimens; RHS; small specimens; small-scale impact testers.

Table of Contents

1. Introduction

Evaluating the mechanical properties of components or structures is typically a destructive approach, since it requires direct material sampling. This is often possible only if the sample size is so small that easy repairing, or even no repairing, is needed for further operation of the component. This is the case of hardness measurements, which can be considered practically nondestructive. This report documents the initial (qualification) phase of a NIST project whose objective is to develop a new standard reference material (SRM): miniaturized Charpy specimens for the indirect verification of small-scale impact testing machines.

Impact test results are needed for the integrity analysis and residual life assessment of reactor pressure vessels, both for current (Generation II) and near-future (Generation III) nuclear power plants. For these reactors, radiation-induced degradation is monitored by means of a surveillance program, which includes testing of standard-size Charpy impact specimens that have been stored in capsules inside the reactor vessels (surveillance capsules). Additional data can be gathered from these surveillance specimens by extracting miniaturized impact specimens from the broken, full-size Charpy specimens. For future advanced nuclear reactors (Gen IV, fusion, accelerator-driven systems), the main restriction is the limited available space for irradiating structural materials under relevant conditions. Miniaturization of the samples, including impact specimens, is therefore an efficient way to optimize both material consumption and irradiation space.

Laboratories testing standard Charpy specimens can indirectly verify their pendulum machines through the use of SRMs provided by national metrology laboratories such as NIST or IRMM (Institute for Reference Materials and Measurements). For laboratories testing miniaturized Charpy specimens with small-scale pendulums (*i.e.*, reduced-scale impact machines with potential energy between 15 J and 50 J and impact speed around 3.8 m/s), no verification specimens are currently available to check the state of calibration of their machines. Past experience with full-size impact machines indicates that without indirect verification, the reliability of the test data and their value for comparison with data from other laboratories is significantly reduced [1-3].

Historically, miniaturized Charpy V-notch (MCVN) specimens have been used since the 1980s in many countries, mainly as a means of re-using already-tested Charpy samples. The non-proportional specimens typically used in Europe are designated KLST (from the German *Kleinstprobe*, or "small specimen") or ESIS (from the acronym of the European Structural Integrity Society) specimens, and have the following nominal dimensions: thickness, 3 mm; width, 4 mm; length, 27 mm; notch depth, 1 mm (*i.e.*, square cross section under the notch); see also Figure 1. Extensive data sets have been generated with this specimen, particularly on nuclear pressure vessel steels [4].

The KLST specimen was the first MCVN type to be included in an international test standard, when in 2006 an amendment (Annex D) titled "Instrumented Charpy V-notch pendulum impact test of sub-size test pieces" was approved for inclusion in the ISO 14556:2000 standard [5].
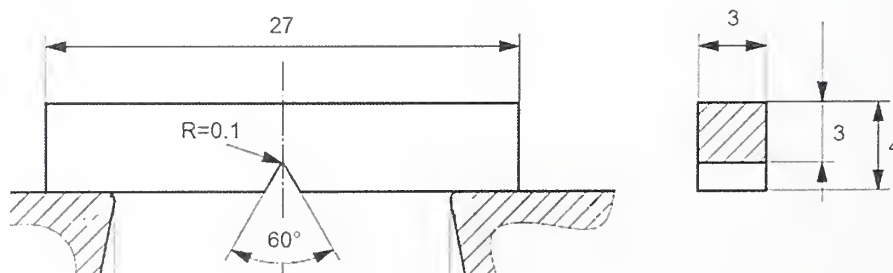

Figure 1 - KLST-type MCVN specimen (dimensions in millimeters).

The proportional (scaled) MCVN specimen preferred in the United States is either the "half-size" (HS) specimen (dimensions 5 mm × 5 mm × 27.5 mm) or the "reduced half-size" (RHS) specimen (4.83 mm × 4.83 mm × 24.13 mm – see Figure 2). The RHS configuration obviously derives from the HS geometry and aims at optimizing the extraction of four MCVN specimens from a broken full-size Charpy half with consideration for the material consumed by the cutting operations. RHS specimens represent the reference MCVN geometry for the ASTM E2248 standard [7], which was officially issued in 2009.
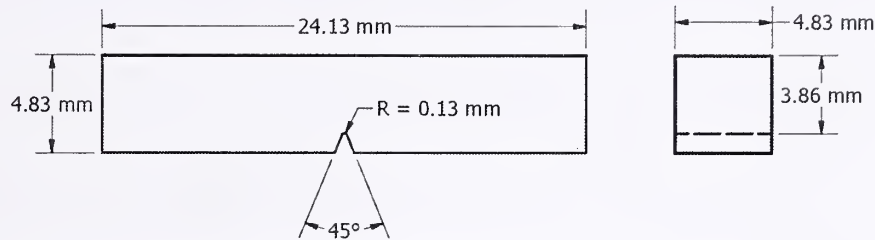
Figure 2 - RHS-type MCVN specimen.

It is important to stress the distinction between miniaturized and sub-size Charpy specimens. The latter are documented in Annex A3 (*Additional Impact Test Specimen Configurations*) of ASTM E23-07a[ε1]. In these specimens, one of the cross-sectional dimensions (either width or thickness) retains the value of full-size samples (10 mm), whereas the other is reduced to 2.5 mm, 3 mm, 5 mm, or 7.5 mm. For the record, this Annex also includes the HS geometry (5 mm × 5 mm cross-section) and an additional 5 mm × 20 mm configuration. Conversely, the MCVN specimens used in this investigation have all linear dimensions reduced with respect to those of a full-size Charpy V-notch (CVN) specimen.

The advanced reactor community, *i.e.*, laboratories working for Generation IV [8] and fusion nuclear reactors, typically uses MCVN specimens for characterizing and qualifying candidate structural materials. In particular, the International Fusion Materials Irradiation Facility (IFMIF) [9], which is expected to closely simulate the irradiation conditions of a fusion power reactor, will have a limited irradiation volume and will therefore rely on the use of very small samples including MCVN specimens. For these advanced reactor applications, codes and regulations have not been developed yet. It is, however, almost certain that small-scale and miniaturized specimens will play a leading role in future regulations, and it would therefore be beneficial to have MCVN SRMs available for consideration as regulations are developed.

Another technical community that would potentially benefit from a more widespread use and public acceptance of MCVN testing is the pipeline community. When product-form dimensions do not allow extraction of full-size Charpy specimens, as in the case of thin-walled pipes or tubes, specimens with reduced size have to be used.

MVCN specimens have also been tested [10] on a conventional, full-size impact tester, provided that anvils and supports are adequately modified to account for specimen span and dimensions. However, the recommended procedure is to use a small-scale pendulum that has a significantly lower potential energy (15 J to 50 J instead of 300 J or more) and slightly lower impact speed (3.8 m/s instead of 5 m/s or more). Testing MCVN specimens on a full-size pendulum can be considered equivalent to using a load cell with 100 kN capacity for testing sub-size tensile specimens that exhibit maximum forces in the order of a few kilonewtons.

Small-scale impact testers cannot be indirectly verified by means of standard Charpy reference specimens, for both dimensional and energy reasons. On the other hand, MCVN specimens with certified values of absorbed

energy or maximum force are currently unavailable. Therefore, users of small-scale impact tester have no means of verifying the performance of their machine by means of an approach equivalent to ASTM E23 or ISO 148-2.

The current project aims at developing and qualifying MCVN reference specimens with certified absorbed energy and maximum force values for both KLST and RHS samples. These objectives will be attained through the following steps:

(a) Establishment of a general procedure for machining MCVN specimens from previously tested NIST reference samples (low, high and super-high energy levels), including dimensional requirements that are stricter than those currently enforced in the ASTM E2248-09 standard.

(b) Initial qualification of the MCVN low, high and super-high reference specimens by performing a statistically relevant number of instrumented tests at NIST with a small-scale pendulum, which has been purchased for this investigation.

(c) Statistical evaluation of the results through the use of qualification procedures similar to those used for CVN samples [3], in order to confirm that MCVN specimens satisfy the requirements for standard reference materials.

(d) Final qualification of the MCVN reference specimens through the organization, coordination and execution of an interlaboratory exercise (Round-Robin) in accordance with ASTM E691-09 [11], involving US and international laboratories.

(e) Statistical evaluation of the Round-Robin results according to ASTM E691-09 [11] and NIST qualification procedures [3].

(f) Establishment of the MCVN indirect verification procedure and the corresponding requirements that users will have to comply with in order to verify their small-scale machine, to be eventually adopted by both ASTM E2248 and ISO 14556 standards.

Additional objectives are:

• The development of data base to demonstrate the usefulness of MCVN specimens for typical pipeline steels.

• Promoting the use of MCVN reference specimens within the communities that represent the most suitable targets (advanced nuclear reactors and pipelines).

Finally, it is worth noting that the feasibility of fabricating MCVN verification specimens of the same materials and energy levels used for existing CVN reference specimens was demonstrated in a collaboration between IRMM (EU reference specimen producer) and SCK•CEN (Belgian Nuclear Center) [12]. Those results justify our decision to use the same materials employed by the Charpy program at NIST for full-size verification specimens.

2. Test equipment

A small-scale impact tester (table-top pendulum machine), equipped with instrumented strikers for testing KLST and RHS specimens, was purchased by the NIST Materials Reliability Division for use in this project.

The parts that need to be changed when testing either MCVN type (KLST or RHS) are the hammer, which includes the instrumented striker, and the supports/anvils block. Weight plates mounted on the hammer are provided to obtain the required potential energy.

The impact energy capacity of the machine, corresponding to a fall angle of 160°, is 50.1 J for KLST and 50.8 for RHS. The nominal impact velocity is 3.5 m/s for both configurations. KLST specimens were tested with a 2 mm striker conforming to ISO 148-2 (Figure 3), while for RHS specimens a scaled-down 8 mm-striker was used in accordance with ASTM E2248 (reduced 4 mm striker, Figure 4).

The nominal distance between specimen supports (span) is 22 mm for KLST and 19.3 mm for RHS.
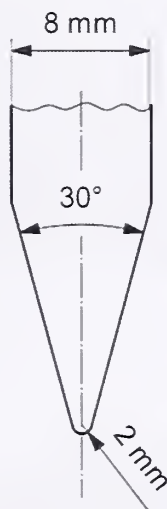
Figure 3 - Dimensions of the KLST striker.
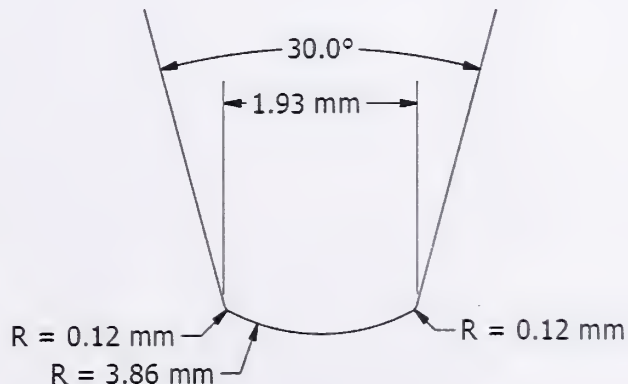
Figure 4 - Dimensions of the RHS striker. The striker width is 8 mm.

The NIST small-scale table-top impact tester is shown in Figure 5 (general view), Figure 6 (detailed view of the hammer and the instrumented striker) and Figure 7 (detailed view of the specimen supports and anvils).

Figure 5 - General view of the NIST small-scale table-top instrumented impact tester.

Instrumented striker
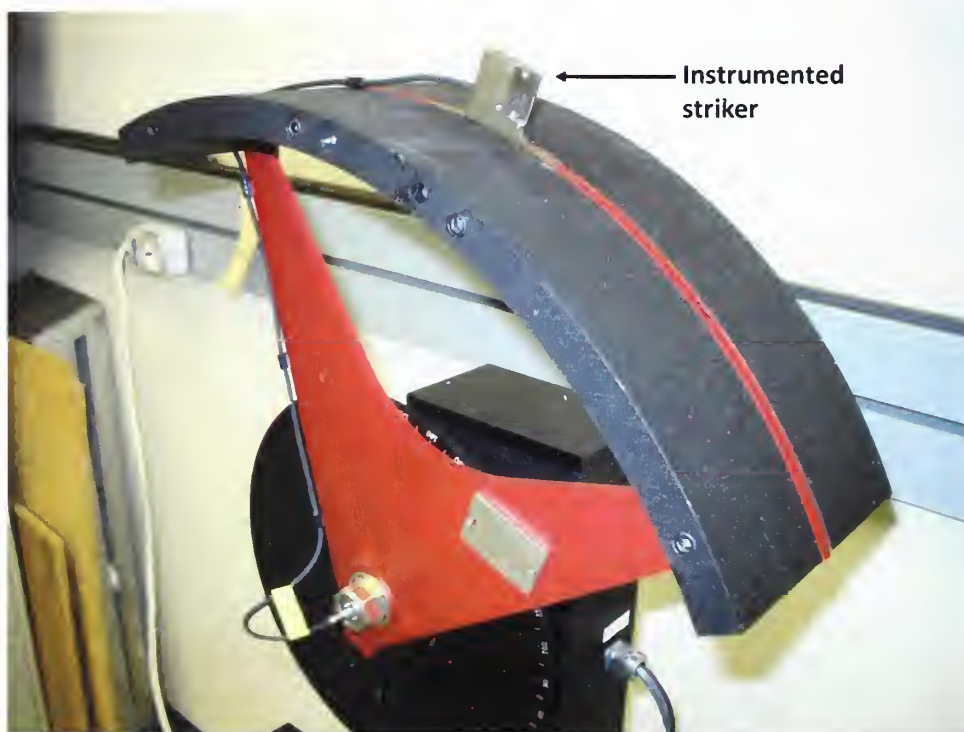
Figure 6 - Detailed view of the hammer and instrumented striker of the NIST small-scale table-top instrumented impact tester.
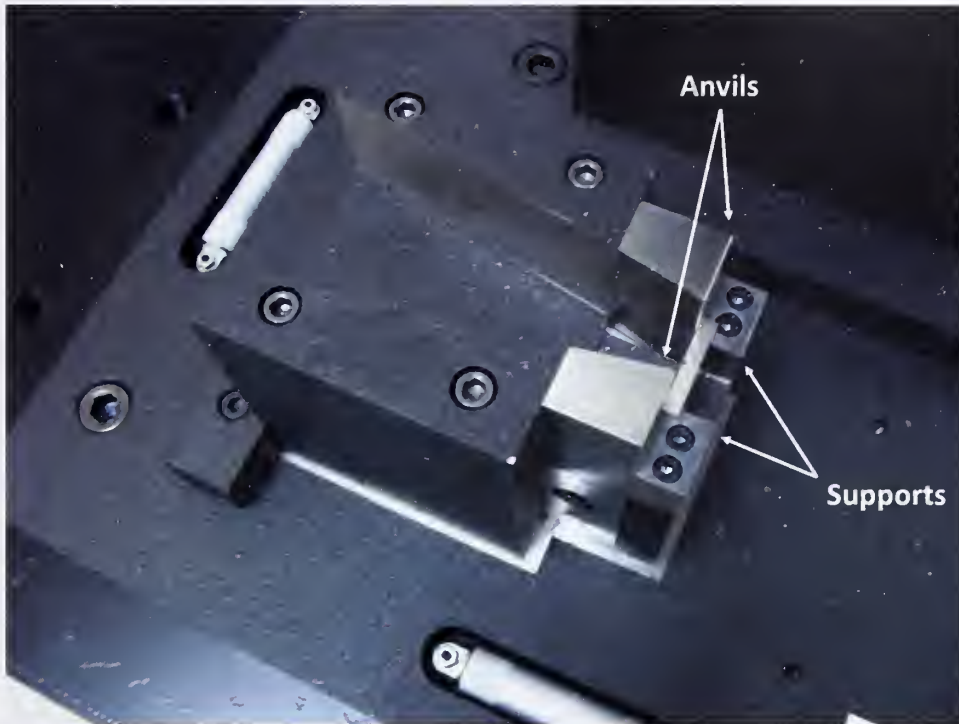
Figure 7 - Detailed view of the supports and anvils of the NIST small-scale table-top instrumented impact tester with a KLST specimen in test position.

The energy absorbed by specimen fracture is calculated from the difference between the fall angle (in the latched position) and the rise angle of the hammer. The angular position of the hammer is monitored by an optical encoder that has an energy resolution of 0.006 J. Values of absorbed energy are corrected for windage and friction; the correction is approximately 0.2 J for both configurations.

Both instrumented strikers were statically calibrated by the manufacturer in accordance with E2248-09 and ISO 14556:2000. The striker voltage/applied force calibration data for both strikers are shown in Figure 8. The KLST striker was calibrated up to an applied compressive force of 3.11 kN (700 lb), while the RHS striker was calibrated up to 10 kN (2250 lb). Both strikers exhibited a fully linear behavior.
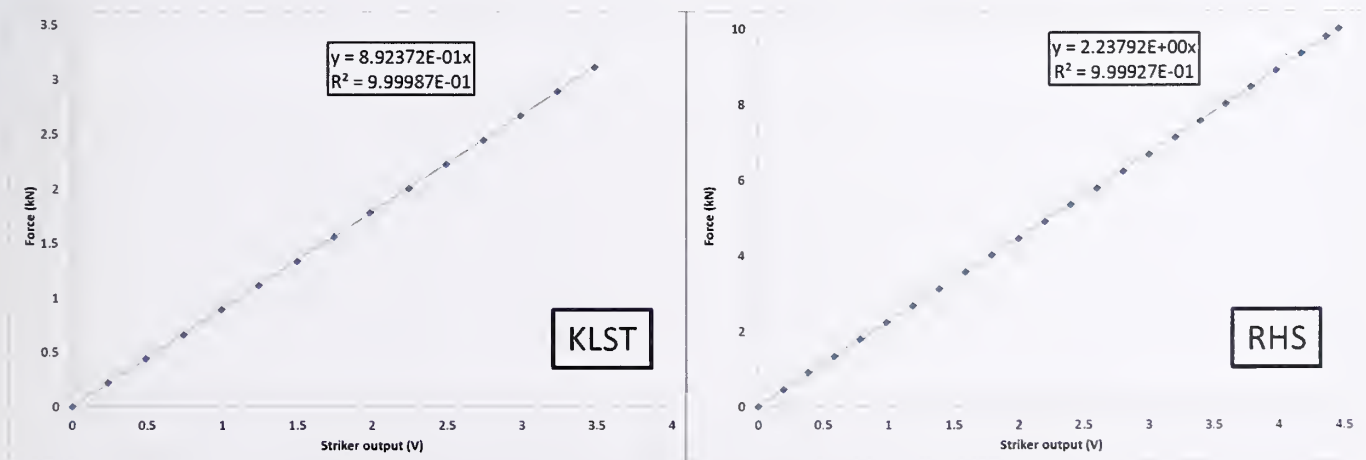
Figure 8 - Static calibration data and linear correlation trend lines for the KLST (left) and RHS (right) instrumented strikers.

The signal of the strain gages from the instrumented strikers is fed through a conditioner stage that amplifies it by a factor 300. The striker signal is then channeled through an analog/digital acquisition unit, which is connected by a USB cable to a computer for time/force data storage and analysis. The sampling rate is 1 MHz. The optical encoder is directly connected to the computer, where the test software converts the readings into values of absorbed energy.

3. Preliminary qualification of NIST small-scale instrumented impact tester: tests on JRQ pressure vessel steel

Before testing MCVN specimens extracted from NIST verification specimens, we performed a preliminary qualification of our test equipment by running KLST instrumented tests on a steel that was used by the ESIS TC5 Working Group for a Round-Robin exercise in the mid-90s [13].

The steel, labeled JRQ, is a reactor pressure vessel steel of the ASTM A533B Cl.1 type, used by the International Atomic Energy Authority (IAEA) as a correlation monitor material in several studies of irradiation-induced material embrittlement [14]. The ESIS TC5 Round-Robin involved 14 international laboratories, who performed instrumented impact tests on KLST specimens of JRQ steel on a number of different tests machines including full-scale and small-scale pendulums, a small-scale drop tower and a high-rate universal testing machine. Phase 1 of the Round-Robin consisted of room temperature tests, whereas in Phase 2 participants performed tests at different temperatures spanning linear elastic, elastic-plastic and ductile-to-brittle transitional behavior for the investigated steel [13]. All the KLST specimens used in the Round-Robin were manufactured from a block designated "ESIS" and distributed to participants by SCK•CEN, the Belgian Nuclear Center.

Thirteen KLST specimens of JRQ steel, from the same lot that had been prepared for the ESIS TC5 Round-Robin, were shipped from SCK•CEN to NIST at the end of 2011. Eight of these were tested at room temperature at NIST, six instrumented and two non-instrumented; the remaining five specimens are kept in storage for future testing.

For every instrumented test performed, values of force F, displacement s and absorbed energy W were determined in accordance with ASTM E2298-09 [15] and ISO 14556:2000 [5] at general yield (subscript gy), maximum force (subscript m), and test termination (subscript t). For both non-instrumented and instrumented tests, values of absorbed energy as measured by the optical encoder, KV, were also recorded. Test results are shown in Table 1, which also reports the ratio between absorbed energies provided by the encoder (KV) and calculated from the area under the force/displacement test record, W_t, as well as the absolute difference between W_t and KV.

Examination of Table 1 reveals that the standard deviation of force values is much lower than that for absorbed energy. The relative scatter of displacement values is intermediate between those of force and energy, except for values at general yield. The ratio KV/W_t between instrumented and encoder energy is extremely consistent, and the absolute difference between KV and W_t ranges between 0.7 J and 0.8 J.

Table 1 - Results of KLST tests performed at NIST on JRQ specimens from the ESIS block. [*]Non-instrumented tests.

Specimen id	T (°C)	F_{gy} (kN)	F_m (kN)	s_{gy} (mm)	s_m (mm)	s_t (mm)	W_m (J)	W_t (J)	KV (J)	KV/W_t	W_t-KV (J)
E519	21	1.01	1.33	0.21	2.18	11.48	2.56	8.08	7.37	0.912	0.71
E520	21	1.02	1.33	0.22	2.02	11.35	2.35	8.77	7.99	0.911	0.78
E542	21	0.99	1.32	0.28	2.14	11.45	2.38	8.69	7.92	0.911	0.77
E545	21	1.01	1.33	0.20	2.07	11.02	2.42	8.49	7.72	0.909	0.77
E546	21	1.02	1.33	0.22	2.07	11.27	2.41	8.44	7.67	0.909	0.77
E547[*]	21	-	-	-	-	-	-	-	7.31	-	-
E548[*]	21	-	-	-	-	-	-	-	7.56	-	-
E549	21	1.01	1.29	0.25	2.04	11.19	2.29	8.79	8.03	0.914	0.76
Average		1.01	1.32	0.23	2.09	11.29	2.21	8.54	7.70	0.911	0.76
Standard deviation		0.01	0.02	0.03	0.06	0.17	0.09	0.27	0.27	0.002	0.03
		1.08 %	1.21 %	12.90 %	2.93 %	1.53 %	3.77 %	3.15 %	3.55 %	0.19 %	3.33 %

NIST data from Table 1 were compared with the results of Phase 1 of the ESIS TC5 Round-Robin (room temperature tests); see Table 2 and Figure 9 to Figure 12.

Table 2 – Comparison between ESIS Round-Robin and NIST results (average and standard deviation). s_r is the repeatability standard deviation according to ASTM E691-11*.

Data set		F_{gy} (kN)	F_m (kN)	s_{gy} (mm)	s_m (mm)	s_t (mm)	W_m (J)	W_t (J)	KV (J)
ESIS R-R [13]	Average	0.98	1.31	0.18	1.91	11.79	2.21	8.35	8.22
	s_r	0.04	0.05	0.04	0.14	1.36	0.22	0.71	0.71
NIST	Average	1.01	1.32	0.23	2.09	11.29 ·	2.40	8.54	7.70
	Standard	0.01	0.02	0.03	0.06	0.17	0.09	0.27	0.27
	deviation	1.08 %	1.21 %	12.90 %	2.93 %	1.53 %	3.77 %	3.15 %	3.55 %

Figure 9 - Instrumented force values: comparison between ESIS Round-Robin and NIST results. The error bars are for the Round-Robin data and correspond to ±2s_r.

---

*ASTM E691-11 definition of s_r : standard deviation of test results obtained under repeatability conditions, *i.e.*, conditions where independent test results are obtained with the same method on identical test items in the same laboratory by the same operator using the same equipment within short intervals of time.
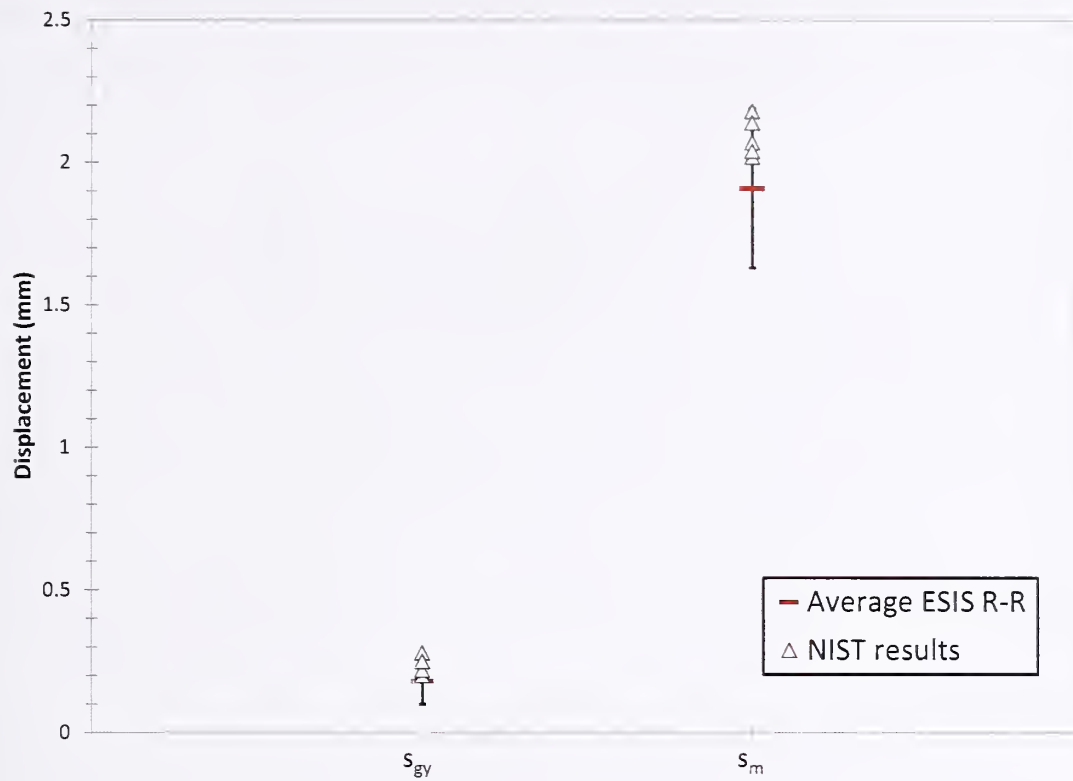
Figure 10 - Instrumented displacement values s_{gy} and s_m: comparison between ESIS Round-Robin and NIST results. The error bars are for the Round-Robin data and correspond to $\pm 2s_r$.
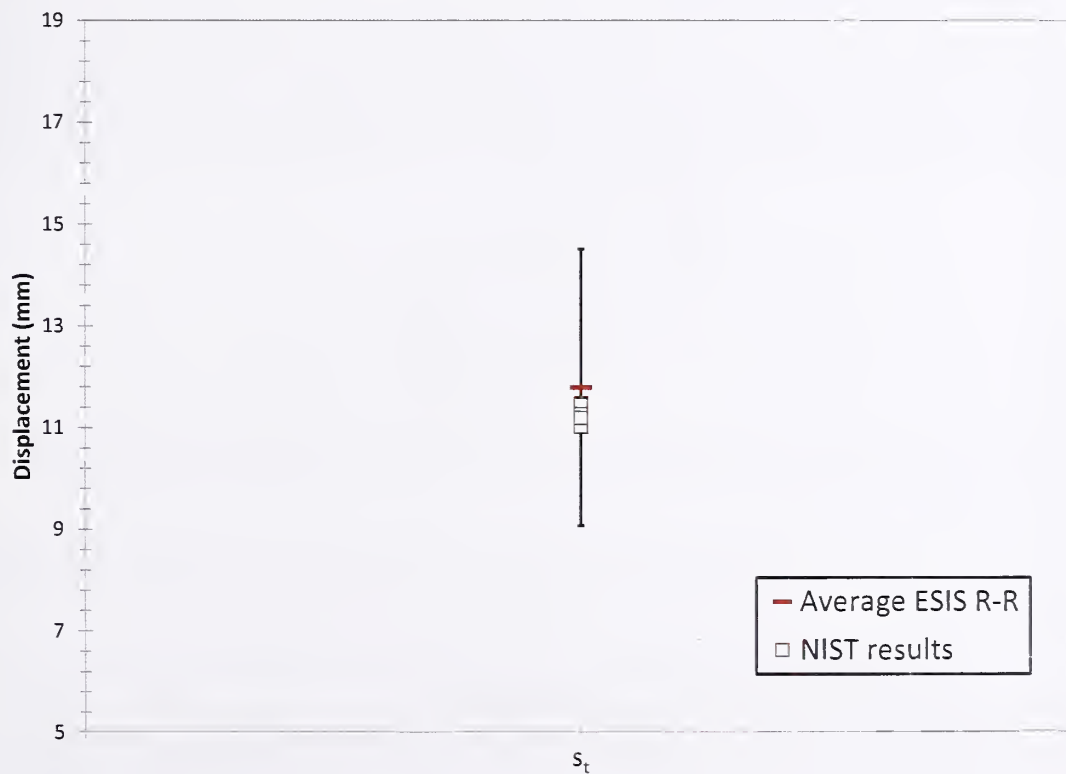
Figure 11 - Instrumented displacement values s_t: comparison between ESIS Round-Robin and NIST results. The error bars are for the Round-Robin data and correspond to $\pm 2s_r$.
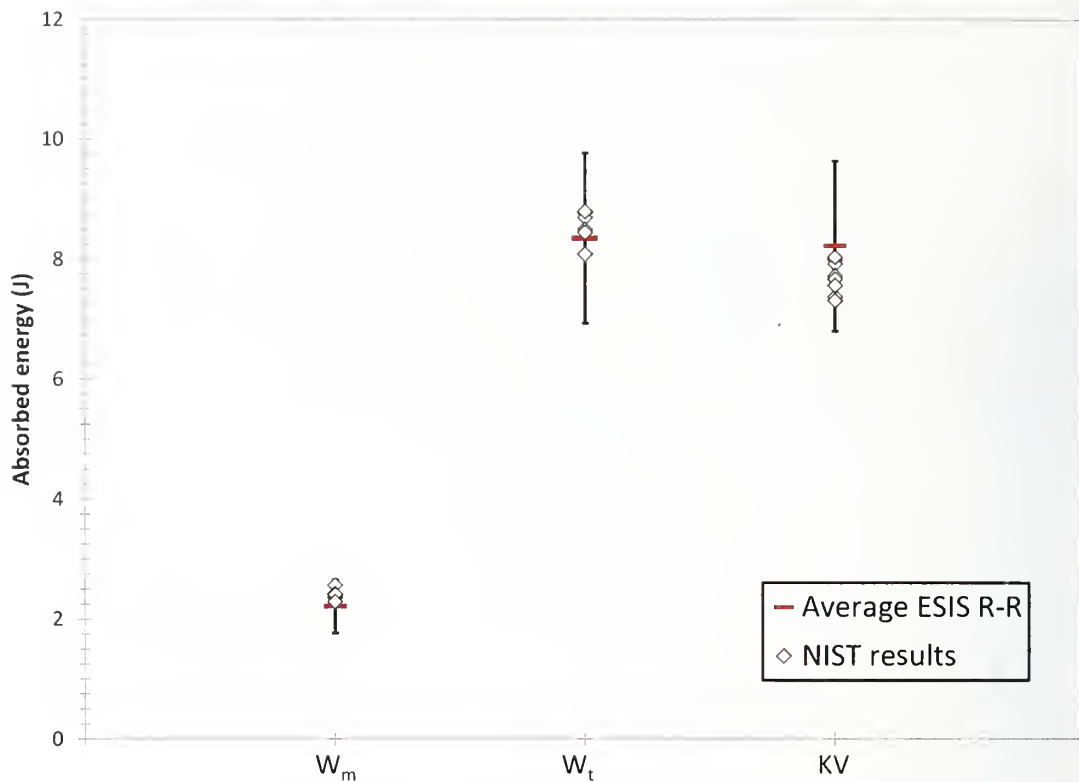
Figure 12 - Instrumented energy values: comparison between ESIS Round-Robin and NIST results. The error bars are for the Round-Robin data and correspond to ±2s_r.

The results obtained at NIST are in excellent agreement with data from the ESIS TC5 Round-Robin, as shown by the comparisons with Round-Robin average values and 98 % confidence intervals (±2s_r). Based on these results, the NIST small-scale instrumented impact tester appears well-suited to perform the tests planned for this project.

4. Development of MCVN SRM's: preliminary testing of low, high and super-high KLST and RHS specimens

4.1 Materials and test matrix

A number of broken (previously tested) full-size NIST verification specimens of different certified energy levels were selected for the fabrication of MCVN specimens.

For the low-energy level, tested specimens from lot LL-103 were selected. This lot has a certified absorbed energy value of 15.3 J (expanded uncertainty 0.1 J) at -40 °C. At the high-energy level, specimens from lot HH-103 were used (certified absorbed energy: 97.5 ± 0.6 J at -40 °C). Both LL-103 and HH-103 are also used as dynamic impact force verification specimens at room temperature (Standard Reference Materials 2113 and 2112, respectively). Their certified values for absorbed energy and maximum force at 21 °C, established through an international round-robin exercise coordinated by NIST [16], are: 18.2 J and 33.00 kN for LL-103 and 105.3 J and 24.06 kN for HH-103. Both SRM 2112 and SRM 2113 are made from 4340 alloy steel.

For the super-high energy level, lot SH-36 was used. Lot SH-36 is made from T200 maraging steel. Its certified energy value at 21 °C is 239.8 J. No certified maximum force value was available, but the average value of 51 CVN instrumented tests performed by NIST at 21 °C on this material for a different study [17] was: $F_m =$ 25.64 kN, with a standard deviation $\sigma = 0.09$ kN. For the same 51 tests, performed on two different machines (TO2 and TO3) equipped with the same instrumented striker, the average value of KV was (239.04 ± 5.97) kN.

For two energy levels (low and high), 32 MCVN specimens for each KLST type (KLST and RHS) were extracted from broken full-size CVN samples. For super-high energy specimens, only eight specimens of each type were machined. The aim of testing super-high MCVN specimens in this preliminary phase was simply to establish whether absorbed energy values were significantly different from those obtained from high energy specimens. From every broken CVN half, four MCVN specimens could be obtained, as shown in Figure 13. As can be seen, the original orientations of the CVN specimen and notch were preserved.
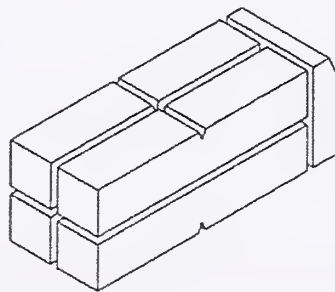
Figure 13 - Sketch of the extraction of four MCVN specimens from one broken CVN half.

The MCVN test matrix for the preliminary qualification phase is shown in Table 3.

Table 3 - Test matrix for the preliminary phase of KLST testing at NIST.

Energy level	Lot	KLST specimens			RHS specimens		
		Non-instrum.	Instrumented	Total	Non-instrum.	Instrumented	Total
Low	LL-103	7	25	32	7	25	32
High	HH-103	7	25	32	7	25	32
Super-High	SH-36	3	5	8	3	5	8

As indicated in Table 3, a few tests were performed non-instrumented.

4.2 Low-energy MCVN test results

Thirty-two KLST specimens and thirty-two RHS specimens from lot LL-103 were tested at room temperature. Force, displacement and absorbed energy results are collected in Table 4 (KLST) and Table 5 (RHS). For each parameter, the tables also provide the average value $\bar{A}$, the absolute standard deviation σ and the percent coefficient of variation CV = $\sigma/\bar{A} \times 100$ %.

In Table 4 and Table 5, the subscripts iu and a indicate brittle fracture and crack arrest, respectively.

Table 4 - NIST test results from KLST specimens of LL-103 (low energy). Specimens 26-32 were tested non-instrumented.

Specimen id	F_{gy} (kN)	F_m (kN)	F_{lu} (kN)	F_a (kN)	s_{gy} (mm)	s_m (mm)	s_{iu} (mm)	s_a (mm)	s_t (mm)	W_{gy} (J)	W_m (J)	W_{iu} (J)	W_a (J)	W_t (J)	KV (J)	KV/W_t	$KV-W_t$ (J)
1	2.21	2.65	2.62	1.31	0.37	0.59	0.59	0.61	0.96	0.44	0.96	0.96	1.00	1.27	1.34	1.055	0.07
2	2.19	2.59	2.59	1.63	0.38	0.60	0.60	0.62	0.97	0.43	0.97	0.97	1.02	1.30	1.41	1.085	0.11
3	2.16	2.62	2.62	1.27	0.37	0.63	0.63	0.69	1.01	0.41	1.04	1.04	1.14	1.33	1.38	1.038	0.05
4	2.13	2.51	2.51	1.44	0.35	0.59	0.59	0.61	1.03	0.39	0.95	0.95	0.99	1.27	1.35	1.063	0.08
5															1.48		
6	2.21	2.64	2.64	1.58	0.39	0.62	0.62	0.65	1.01	0.46	1.01	1.01	1.09	1.36	1.43	1.051	0.07
7	2.20	2.61	2.57	1.53	0.36	0.60	0.63	0.65	1.05	0.41	1.02	1.10	1.14	1.40	1.46	1.043	0.06
8	2.17	2.65	2.65	1.54	0.37	0.60	0.60	0.62	1.02	0.41	0.98	0.98	1.03	1.30	1.36	1.046	0.06
9	2.19	2.63	2.59	1.45	0.36	0.62	0.63	0.66	0.93	0.42	1.05	1.08	1.15	1.37	1.44	1.051	0.07
10	2.18	2.56	2.56	1.34	0.37	0.58	0.58	0.60	0.96	0.42	0.91	0.91	0.95	1.22	1.29	1.057	0.07
11	2.15	2.58	2.53	1.59	0.37	0.62	0.65	0.67	1.02	0.40	1.02	1.10	1.15	1.39	1.45	1.043	0.06
12	2.16	2.57	2.57	1.14	0.35	0.56	0.56	0.59	0.94	0.41	0.92	0.92	0.96	1.22	1.30	1.066	0.08
13	2.16	2.65	2.60	1.28	0.37	0.62	0.63	0.66	1.01	0.42	1.03	1.05	1.12	1.33	1.39	1.045	0.06
14	2.12	2.64	2.64	1.17	0.38	0.63	0.63	0.67	1.09	0.38	1.00	1.00	1.10	1.32	1.39	1.053	0.07
15	2.24	2.50	2.50	1.48	0.37	0.56	0.56	0.61	0.93	0.46	0.93	0.93	0.99	1.21	1.25	1.033	0.04
16	2.12	2.57	2.57	1.56	0.37	0.59	0.59	0.64	1.03	0.42	0.92	0.92	1.01	1.25	1.34	1.072	0.09
17	2.19	2.64	2.64	1.12	0.37	0.61	0.61	0.63	0.97	0.42	1.00	1.00	1.04	1.28	1.37	1.070	0.09
18	2.03	2.51	2.51	1.44	0.35	0.57	0.57	0.62	0.94	0.37	0.86	0.86	0.95	1.18	1.28	1.085	0.10
19	2.18	2.66	2.66	1.22	0.37	0.59	0.59	0.61	0.95	0.43	0.95	0.95	0.99	1.25	1.33	1.064	0.08
20	2.20	2.61	2.61	1.56	0.36	0.57	0.57	0.59	0.87	0.42	0.91	0.91	0.96	1.19			
21	2.18	2.58	2.58	1.29	0.38	0.63	0.63	0.66	1.00	0.43	1.03	1.03	1.09	1.33	1.39	1.045	0.06
22	2.16	2.61	2.51	1.23	0.37	0.62	0.63	0.65	0.92	0.41	1.00	1.03	1.07	1.28	1.37	1.070	0.09
23	2.18	2.58	2.58	1.31	0.37	0.61	0.61	0.63	0.98	0.41	1.01	1.01	1.05	1.27	1.34	1.055	0.07
24	2.15	2.57	2.57	1.41	0.37	0.61	0.61	0.63	1.14	0.40	0.97	0.97	1.01	1.32	1.41	1.068	0.09
25	2.16	2.61	2.52	1.24	0.37	0.61	0.62	0.65	1.00	0.43	1.00	1.03	1.09	1.34	1.43	1.067	0.09
26															1.33		
27															1.33		
28															1.29		
29															1.42		
30															1.39		
31															1.27		
32																	
N	24	24	24	24	24	24	24	24	24	24	24	24	24	24	30	23	23
Average	2.17	2.60	2.58	1.38	0.37	0.60	0.61	0.63	0.99	0.42	0.98	0.99	1.05	1.29	1.37	1.058	0.07
σ (abs)	0.041	0.046	0.049	0.156	0.010	0.022	0.026	0.027	0.058	0.021	0.049	0.063	0.067	0.061	0.060	0.014	0.017
CV	1.9%	1.8%	1.9%	11.3%	2.6%	3.6%	4.2%	4.3%	5.9%	5.0%	5.1%	6.4%	6.4%	4.7%	4.4%	1.3%	22.5%

NOTE – N is the number of available data. Instrumented data for specimen 5 were lost because the acquisition system did not trigger. The values of KV for specimens 20 and 32 were lost because the optical encoder did not trigger.

13

Table 5 - NIST test results from RHS specimens of LL-103 (low energy). Specimens 26-32 were tested non-instrumented.

Specimen id	F_{gy} (kN)	F_m (kN)	F_{iu} (kN)	F_a (kN)	s_{gy} (mm)	s_m (mm)	s_{iu} (mm)	s_a (mm)	s_t (mm)	W_{gy} (J)	W_m (J)	W_{iu} (J)	W_a (J)	W_t (J)	KV (J)	KV/W_t	$KV-W_t$ (J)
1	6.06	8.20	8.20	2.35	0.25	0.52	0.52	0.55	0.71	0.81	2.75	2.75	2.93	3.18	3.27	1.028	0.09
2	5.98	8.24	8.12	1.55	0.25	0.54	0.55	0.59	0.96	0.78	2.90	2.98	3.20	3.50	3.55	1.014	0.05
3	6.51	8.21	8.21	3.21	0.28	0.55	0.55	0.58	1.83	0.96	2.96	2.96	3.14	3.79	3.56	0.939	-0.23
4	6.02	8.26	8.26	2.83	0.26	0.53	0.53	0.56	0.83	0.77	2.79	2.79	2.98	3.30	3.31	1.003	0.01
5	5.93	8.21	7.73	3.35	0.26	33.88	0.50	0.53	0.88	0.75	2.35	2.51	2.69	3.07	3.09	1.007	0.02
6	6.09	8.13	8.13	3.21	0.25	0.53	0.53	0.56	1.83	0.81	2.83	2.83	3.02	3.70	3.45	0.932	-0.25
7	5.91	8.16	8.16	2.97	0.26	0.54	0.54	0.57	0.72	0.73	2.81	2.81	3.00	3.26	3.37	1.034	0.11
8	6.06	8.10	8.10	1.87	0.25	0.53	0.53	0.56	0.91	0.79	2.83	2.83	2.99	3.31	3.29	0.994	-0.02
9	6.06	8.30	8.30	2.00	0.25	0.53	0.53	0.57	0.92	0.77	2.88	2.88	3.11	3.44	3.45	1.003	0.01
10	6.03	8.42	8.42	1.93	0.24	0.52	0.52	0.56	0.71	0.74	2.86	2.86	3.11	3.33	3.39	1.018	0.06
11	6.41	8.22	8.22	2.29	0.30	0.59	0.59	0.62	1.88	0.92	3.09	3.09	3.25	3.91	3.65	0.934	-0.26
12	5.97	8.34	8.16	2.12	0.25	0.54	0.55	0.60	1.87	0.77	2.87	2.96	3.26	4.01	3.74	0.933	-0.27
13	5.07	8.29	8.29	3.03	0.23	0.51	0.51	0.54	1.81	0.78	2.82	2.82	3.00	3.63	3.44	0.948	-0.19
14	6.08	8.03	8.03	2.11	0.25	0.53	0.53	0.56	1.82	0.80	2.83	2.83	2.99	3.65	3.44	0.942	-0.21
15	5.96	7.86	7.83	2.91	0.25	0.49	0.50	0.53	0.88	0.75	2.50	2.58	2.75	3.11	3.11	1.000	0.00
16	5.93	7.98	7.89	2.89	0.25	0.49	0.51	0.54	1.81	0.77	2.46	2.62	2.80	3.42	3.44	1.006	0.02
17	6.01	8.27	8.01	2.16	0.29	0.56	0.57	0.60	1.85	0.84	2.86	2.94	3.10	3.65	3.42	0.937	-0.23
18	6.13	7.98	7.98	1.76	0.24	0.51	0.51	0.54	0.89	0.81	2.77	2.77	2.92	3.23	3.20	0.991	-0.03
19	6.15	8.27	8.05	1.53	0.25	0.55	0.56	0.59	0.75	0.78	3.08	3.16	3.31	3.54	3.55	1.003	0.01
20	5.98	8.04	8.04	1.69	0.25	0.50	0.50	0.54	0.88	0.75	2.60	2.60	2.83	3.16	3.13	0.991	-0.03
21	6.09	8.13	7.91	2.30	0.25	0.51	0.52	0.55	1.82	0.76	2.69	2.78	2.93	3.61	3.39	0.939	-0.22
22	6.05	8.27	8.27	2.06	0.26	0.54	0.54	0.58	1.52	0.80	2.84	2.84	3.08	3.60	3.44	0.956	-0.16
23	6.04	8.41	8.41	1.68	0.25	0.53	0.53	0.57	0.71	0.80	2.84	2.84	3.08	3.30	3.34	1.012	0.04
24	6.01	8.12	8.12	2.66	0.25	0.52	0.52	0.55	0.70	0.79	2.73	2.73	2.91	3.16	3.26	1.032	0.10
25	6.06	8.07	8.07	2.22	0.26	0.53	0.53	0.56	0.91	0.78	2.80	2.80	2.96	3.31	3.29	0.994	-0.02
26															3.43		
27															3.40		
28															3.61		
29															3.71		
30															3.65		
31															3.52		
32															3.67		
N	25	25	25	25	25	25	25	25	25	25	25	25	25	25	32	25	25
Average	6.06	8.18	8.12	2.35	0.26	1.86	0.53	0.56	1.22	0.79	2.79	2.82	3.01	3.45	3.38	0.984	-0.06
σ (abs)	0.135	0.137	0.170	0.562	0.015	6.670	0.022	0.023	0.499	0.051	0.169	0.149	0.156	0.255	0.161	0.035	0.129
CV	2.2%	1.7%	2.1%	24.0%	5.9%	358.1%	4.2%	4.1%	41.1%	6.5%	6.1%	5.3%	5.2%	7.4%	4.8%	3.6%	-202.3%

NOTE – N is the number of available data.

The variation of MCVN results was compared to the scatter resulting from room temperature pilot lot tests with the three NIST reference machines (TO2, TK and TO3). The coefficients of variation for KV measured from the three machines on the basis of 30, 25 and 25 tests, respectively, are: 3.75 % (TO2), 3.46 % (TK) and 2.22 % (TO3). The corresponding CV values from KLST and RHS tests, 4.4 % and 4.8 %, are slightly higher. Note that the coefficients of variation for absorbed energy calculated from the instrumented force/displacement curves (W_t) are higher for both KLST tests (4.7 %) and RHS tests (7.4 %). On the other hand, force-based parameters from MCVN tests have lower CV values (about 2 %), with the exception of arrest forces F_a.

4.2.1 Calculation of sample size and outlier analysis

The sample size, n, is the minimum number of specimens from a given production lot that should be tested in a verification test [18]. It is calculated as:

$$n = \left(\frac{3 s_p}{E} \right)^2 \quad , \tag{1}$$

where s_p is the pooled standard deviation (or the machine standard deviation if only one machine is used), and E is the greatest of 0.105 J (KLST) or 0.263 J (RHS)[†] and 5 % of the mean absorbed energy. For KLST and RHS specimens of LL-103, the sample size is 2.9 and 3.8, respectively. For comparison, the testing of the pilot lot of LL-103 full-size specimens returned a sample size of 1.3 at -40 °C and 1.6 at room temperature.

The outlier analysis is conventionally performed by means of box-and-whiskers plots to provide a graphical summary of the data and identify outliers, defined as values that are lower than the first quartile or higher than the third quartile by more than 1.5 times the absolute difference between the first and third quartiles. If a lot has more than 5 % outliers, it may be rejected [18]. It is important to note than a specimen identified as an outlier is not removed from the analysis, unless it shows physical evidence of jamming, material flaws, or other atypical behavior. Box-and-whiskers plots for KV values are shown in Figure 14 (KLST) and Figure 15 (RHS). No outliers were detected.
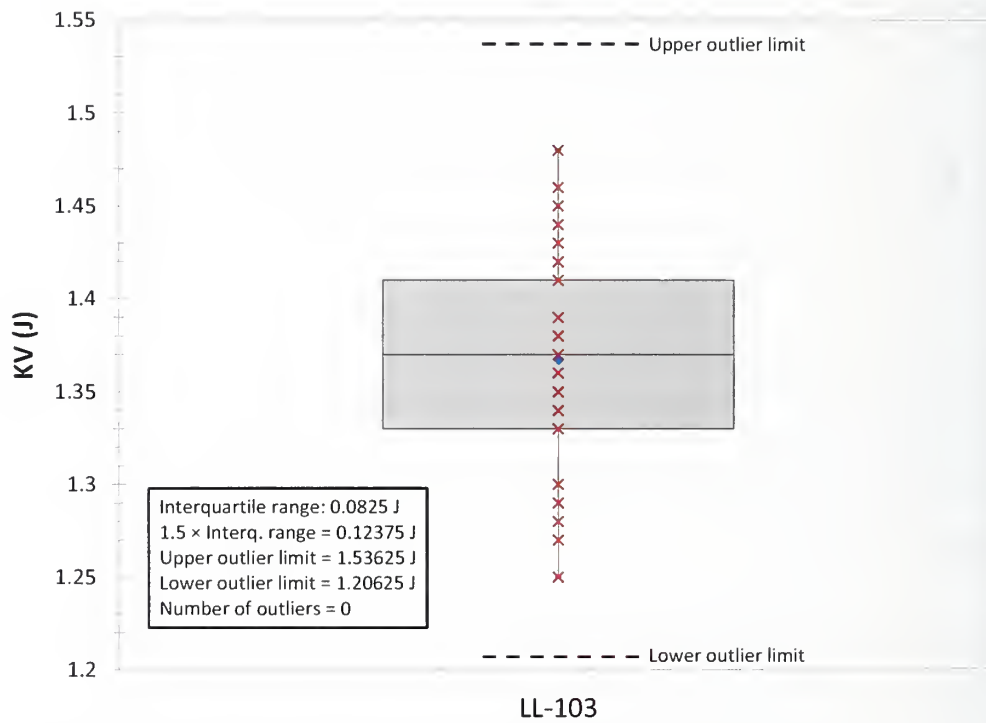
Figure 14 - Box-and-whisker plot for KV values from KLST specimens of LL-103.

In addition to the box-and-whiskers plot method, the outlier analysis was also conducted according to Grubbs' test, also known as the maximum normed residual test or the extreme studentized deviate method [19]. This statistical test is used for data sets that are assumed to come from a normally distributed population, and should not be used for sample sizes of six or less. Grubbs' test detects one outlier at a time, and should be repeated once the first outlier (if detected) is expunged from the data set.

[†]The NIST procedure for standard Charpy specimens [18] uses the greater between 1.4 J and 5 % of KV for the factor E in Eq. (1). In this study, the value 1.4 J was normalized by the ratio between $KV_{\text{full-size}}$ and $KV_{\text{sub-size}}$ for the specific energy level and MCVN type, i.e., 13.34 for KLST and 5.33 for RHS at the low energy level (see section 5.2).

Grubbs' test was applied to values of F_{gy}, F_m, W_m, W_t and KV and calculated from the tests performed. Outlier detection was carried out at a significance level $\alpha = 0.01$. The results for MCVN specimens of LL-103 are summarized in Table 6.
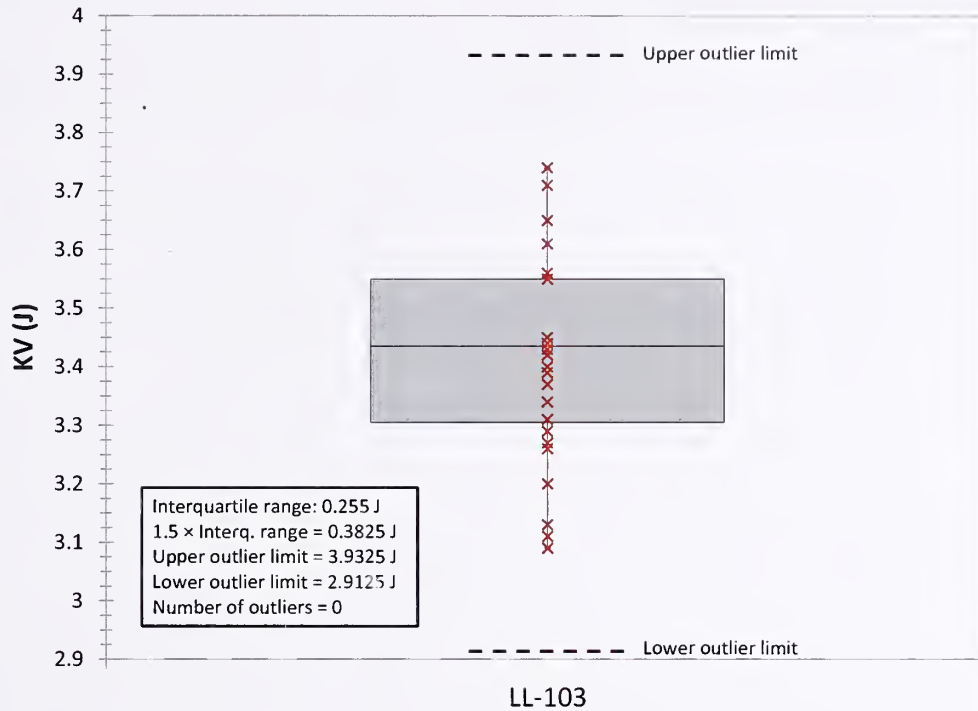

Figure 15 - Box-and-whisker plot for *KV* values from RHS specimens of LL-103.

Table 6 - Results of Grubbs' test for the detection of outliers on MCVN tests of LL-103. *N* is the number of values analyzed.

Specimen type	Parameter	N	Outliers detected	Outlier specimens[‡]
KLST	F_{gy}	24	1	18
	F_m	24	0	-
	W_m	24	0	-
	W_t	24	0	-
	KV	30	0	-
RHS	F_{gy}	25	2	3,11[§]
	F_m	25	0	-
	W_m	25	0	-
	W_t	25	0	-
	KV	32	0	-

Outliers were detected only for forces at general yield. This is not surprising, considering the intrinsic subjectivity of the determination of the general yield point from the instrumented test record. For *KV* values, the

---

[‡] See Table 4 (KLST) and Table 5 (RHS) for specimen numbers.
[§] The two outliers were detected in two successive runs of Grubbs' test.

outcome of the Grubbs' test confirms the results of the box-and-whisker method (*i.e.*, no outliers detected at α = 0.01).

4.3   High-energy MCVN test results

Thirty-two KLST specimens and thirty-two RHS specimens from lot HH-103 were tested at room temperature. Force, displacement and absorbed energy results are collected in Table 7 (KLST) and Table 8 (RHS).

Table 7 - NIST test results from KLST specimens of HH-103 (high energy). Specimens 26-32 were tested non-instrumented.

Specimen id	F_{gy} (kN)	F_m (kN)	s_{gy} (mm)	s_m (mm)	s_t (mm)	W_{gy} (J)	W_m (J)	W_t (J)	KV (J)	KV/W_t	W_t-KV (J)
1	1.49	1.91	0.28	0.65	12.35	0.21	0.86	5.77	5.09	0.882	0.68
2	1.50	1.92	0.26	0.63	13.10	0.21	0.87	5.95	5.25	0.882	0.70
3	1.51	1.94	0.28	0.64	11.68	0.22	0.87	5.96	5.29	0.888	0.67
4	1.51	1.92	0.27	0.62	12.22	0.21	0.85	5.85	5.15	0.880	0.70
5	1.50	1.90	0.29	0.66	12.13	0.21	0.89	5.70	5.00	0.877	0.70
6	1.49	1.91	0.27	0.64	12.20	0.23	0.86	5.91	5.13	0.868	0.78
7	1.53	1.92	0.27	0.62	11.49	0.24	0.86	6.02	5.31	0.882	0.71
8	1.50	1.90	0.26	0.63	11.59	0.20	0.88	6.03	5.28	0.876	0.75
9	1.50	1.90	0.28	0.63	12.18	0.21	0.83	5.81	5.11	0.880	0.70
10	1.49	1.91	0.27	0.64	12.17	0.21	0.86	5.86	5.13	0.875	0.73
11	1.51	1.92	0.26	0.62	12.18	0.21	0.85	6.14	5.38	0.876	0.76
12	1.49	1.93	0.26	0.62	11.41	0.20	0.86	5.92	5.26	0.889	0.66
13	1.48	1.92	0.28	0.65	12.19	0.20	0.87	5.84	5.12	0.877	0.72
14	1.48	1.90	0.27	0.63	11.66	0.21	0.86	5.78	5.10	0.882	0.68
15	1.49	1.91	0.28	0.64	11.47	0.21	0.86	5.99	5.34	0.891	0.65
16	1.54	1.93	0.28	0.65	12.37	0.22	0.89	5.79	5.10	0.881	0.69
17	1.51	1.93	0.28	0.63	12.29	0.22	0.86	5.94	5.18	0.872	0.76
18	1.52	1.91	0.28	0.63	12.11	0.22	0.86	6.11	5.33	0.872	0.78
19	1.49	1.91	0.28	0.64	12.20	0.21	0.86	5.88	5.14	0.874	0.74
20	1.52	1.93	0.28	0.65	11.59	0.21	0.88	6.03	5.28	0.876	0.75
21	1.45	1.90	0.26	0.63	11.50	0.20	0.86	5.87	5.21	0.888	0.66
22	1.49	1.91	0.26	0.62	12.18	0.20	0.85	5.74	5.10	0.889	0.64
23	1.54	1.92	0.28	0.63	11.65	0.25	0.85	5.76	5.10	0.885	0.66
24	1.52	1.91	0.29	0.65	12.20	0.23	0.88	5.93	5.18	0.874	0.75
25	1.61	1.93	0.33	0.67	11.52	0.26	0.89	6.08	5.34	0.878	0.74
26									5.13		
27									5.15		
28									5.35		
29									5.36		
30									5.17		
31									5.29		
32									5.06		
N	25	25	25	25	25	25	25	25	32	25	25
Average	1.51	1.92	0.28	0.64	11.99	0.22	0.86	5.91	5.20	0.880	0.71
σ (abs)	0.029	0.012	0.015	0.013	0.406	0.016	0.014	0.120	0.104	0.006	0.042
CV	2.0%	0.6%	5.3%	2.1%	3.4%	7.2%	1.7%	2.0%	2.0%	0.7%	5.9%

The coefficients of variation for *KV* values obtained from the pilot lot testing of HH-103 on the three NIST reference machines were: 2.47 % (TO2), 2.64 % (TK) and 2.30 % (TO3). Twenty-five full-size Charpy specimens were tested on each machine. The corresponding CV values from KLST and RHS tests, 2.0 % and 2.6 %, respectively, are fully comparable. Unlike low-energy MCVN tests, the coefficients of variation for instrumented absorbed energies (W_t) are the same for KLST tests (2.0 %) and lower for RHS tests (2.2 %). Forces at general yield (F_{gy}) have comparable values of CV (about 2 %), while maximum force values (F_m) exhibit very low variability (CV = 0.6 %).

Table 8 - NIST test results from RHS specimens of HH-103 (high energy). Specimens 26-32 were tested non-instrumented.

Specimen id	F_{gy} (kN)	F_m (kN)	s_{gy} (mm)	s_m (mm)	s_t (mm)	W_{gy} (J)	W_m (J)	W_t (J)	KV (J)	KV/W_t	W_t-KV (J)
1	5.00	6.34	0.20	0.92	29.29	0.52	4.84	16.14	14.45	0.895	1.69
2	5.45	6.39	0.26	0.93	29.24	0.71	4.84	16.28	14.56	0.894	1.72
3	5.28	6.41	0.25	0.91	29.30	0.65	4.71	16.12	14.40	0.893	1.72
4	5.40	6.30	0.26	0.88	29.44	0.70	4.47	15.70	14.32	0.912	1.38
5	5.36	6.39	0.25	0.92	29.31	0.70	4.75	16.09	14.41	0.896	1.68
6	5.40	6.43	0.24	0.95	28.62	0.68	5.07	17.19	15.60	0.908	1.59
7	5.23	6.39	0.24	0.93	10.30	0.64	4.80	16.45			
8	5.34	6.36	0.25	0.91	29.30	0.68	4.66	16.08	14.51	0.902	1.57
9	5.46	6.38	0.27	0.89	29.33	0.72	4.54	15.99	14.56	0.911	1.43
10	5.37	6.35	0.24	0.88	29.52	0.67	4.58	15.49	13.78	0.890	1.71
11	5.34	6.29	0.24	0.88	29.40	0.71	4.53	15.77	14.39	0.912	1.38
12	5.37	6.32	0.24	0.90	29.13	0.67	4.70	16.51	14.99	0.908	1.52
13	5.32	6.41	0.24	0.93	29.29	0.65	4.89	16.17	14.41	0.891	1.76
14	5.43	6.33	0.28	0.94	29.41	0.71	4.70	15.73	14.15	0.900	1.58
15	5.39	6.41	0.27	0.92	29.37	0.70	4.64	15.95	14.26	0.894	1.69
16	5.52	6.39	0.31	0.96	27.39	0.84	4.84	16.61	15.05	0.906	1.56
17	5.36	6.39	0.25	0.91	29.38	0.71	4.64	15.90	14.24	0.896	1.66
18	5.37	6.37	0.26	0.90	29.44	0.71	4.58	15.75	14.11	0.896	1.64
19	5.38	6.38	0.27	0.94	29.27	0.74	4.85	16.16	14.73	0.912	1.43
20	5.38	6.44	0.26	0.96	29.20	0.72	4.98	16.36	14.67	0.897	1.69
21	5.39	6.38	0.25	0.90	29.29	0.75	4.62	16.10	14.66	0.911	1.44
22	5.40	6.36	0.26	0.91	10.56	0.69	4.68	16.13	14.74	0.914	1.39
23	5.46	6.39	0.24	0.87	29.35	0.73	4.55	15.92	14.51	0.911	1.41
24	5.55	6.43	0.21	0.83	29.22	0.74	4.60	16.29	14.69	0.902	1.60
25	5.34	6.30	0.25	0.89	29.47	0.66	4.48	15.68	14.01	0.893	1.67
26									14.48		
27									14.25		
28									14.56		
29									14.12		
30									14.07		
31									14.43		
32									15.23		
N	25	25	25	25	25	25	25	25	31	24	24
Average	5.37	6.37	0.25	0.91	27.71	0.70	4.70	16.10	14.49	0.902	1.58
σ (abs)	0.103	0.041	0.021	0.030	5.218	0.055	0.155	0.358	0.371	0.008	0.126
CV	1.9%	0.6%	8.5%	3.3%	18.8%	7.9%	3.3%	2.2%	2.6%	0.9%	8.0%

NOTE – The value of KV for specimen 7 was lost because the optical encoder did not trigger.

4.3.1   Calculation of sample size and outlier analysis

The sample size calculated from HH-103 MCVN test results according to Eq. (1) is $n = 1.4$ for KLST specimens and $n = 2.4$ for RHS specimens[**]. For comparison, the values of sample size returned from the pilot lot testing of HH-103 full-size specimens were 2.3 at -40 °C and 2.2 at room temperature.

The outlier analysis for KV values performed by means of box-and-whiskers plots, shown in Figure 14 (KLST) and Figure 15 (RHS), detected one outlier among the RHS specimens (sample 6). No evidence of jamming or other atypical occurrences were associated to this specimen. However, the percentage of outliers (1/31, or 3.2 %) is well below the 5 % threshold for potential lot rejection [18].

[**]The NIST procedure for standard Charpy specimens [18] uses the greater between 1.4 J and 5 % of KV in Eq. (1). The value 1.4 J was normalized by the ratio between $KV_{full-size}$ and $KV_{sub-size}$ for the specific energy level and MCVN type, *i.e.*, 20.26 for KLST and 7.28 for RHS at the high-energy level (see section 5.2).
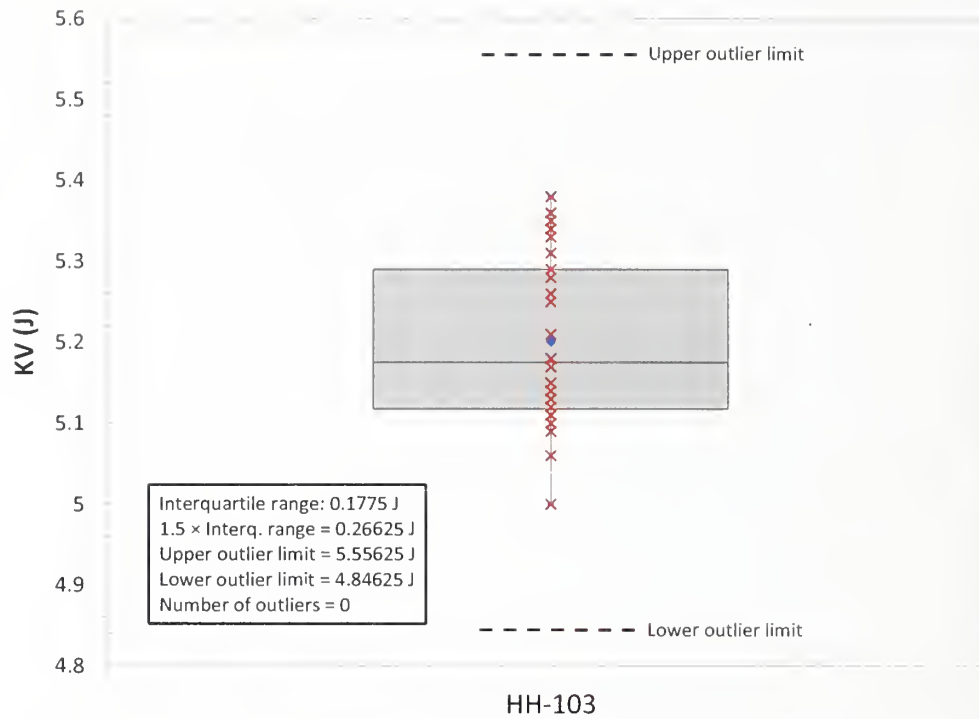
Figure 16 - Box-and-whisker plot for *KV* values from KLST specimens of HH-103.
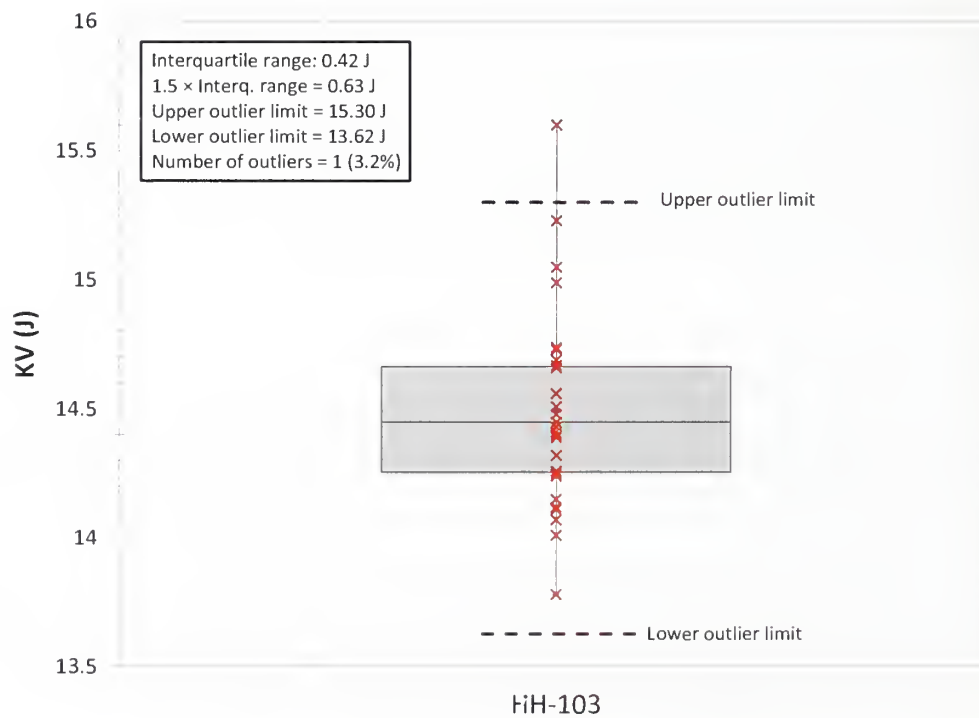

Figure 17 - Box-and-whisker plot for *KV* values from RHS specimens of HH-103.

The results of the outlier analysis conducted by means of Grubbs' test are summarized in Table 9.

19

Table 9 - Results of Grubbs' test for the detection of outliers on MCVN tests of HH-103.

Specimen type	Parameter	N	Outliers detected	Outlier specimens[††]
KLST	F_{gy}	25	1	25
	F_m	25	0	-
	W_m	25	0	-
	W_t	25	0	-
	KV	32	0	-
RHS	F_{gy}	25	1	1
	F'_m	25	0	-
	W_m	25	0	-
	W_t	25	0	-
	KV	32	0	-

Again, outliers were detected only for F_{gy} values. In this case, the outcome of Grubbs' test for KV values from RHS tests does not coincide with the results of the box-and-whisker method. The outlier detected by the latter method (specimen 6, $KV = 15.60$ J) is not classified as an outlier by Grubbs' test. For this test, the Z value is maximum (2.98), but remains below the critical value (3.25) at the $\alpha = 0.01$ significance level. Note, however, that if Grubbs' test is performed at a significance level $\alpha = 0.05$, the threshold value becomes 2.92 and specimen 6 is then also detected as an outlier.

4.4   Super high-energy MCVN test results

Only eight KLST specimens and eight RHS specimens from lot SH-36 were tested at room temperature. Additional tests are planned in the continuation of this project, so that an equivalent number of test results are available for each energy level and specimen configuration. Force, displacement and absorbed energy results are collected in Table 10 (KLST) and Table 11 (RHS), as well as average values, absolute standard deviations and percent coefficients of variation.

Table 10 - NIST test results from KLST specimens of SH-36 (super-high energy). Specimens 6-8 were tested non-instrumented.

Specimen id	F_{gy} (kN)	F_m (kN)	s_{gy} (mm)	s_m (mm)	s_t (mm)	W_{gy} (J)	W_m (J)	W_t (J)	KV (J)	KV/W_t	W_t-KV (J)
1	1.66	1.96	0.36	1.40	11.10	0.31	2.25	10.89	9.77	0.897	1.12
2	1.65	1.96	0.37	1.40	11.19	0.30	2.24	10.74	9.64	0.898	1.10
3	1.65	1.97	0.33	1.40	11.34	0.27	2.27	10.84	9.72	0.897	1.12
4	1.67	1.99	0.35	1.40	10.97	0.29	2.28	11.11	9.98	0.898	1.13
5	1.65	1.96	0.33	1.38	11.04	0.28	2.24	10.66	9.60	0.901	1.06
6									9.16		
7									9.57		
8									9.81		
N	5	5	5	5	5	5	5	5	8	5	5
Average	1.66	1.97	0.35	1.40	11.13	0.29	2.26	10.85	9.66	0.898	1.11
σ (abs)	0.009	0.013	0.018	0.009	0.143	0.016	0.018	0.171	0.240	0.002	0.028
CV	0.5%	0.7%	5.1%	0.6%	1.3%	5.5%	0.8%	1.6%	2.5%	0.2%	2.5%

[††] See Table 7 (KLST) and Table 8 (RHS) for specimen numbers.

Table 11 - NIST test results from RHS specimens of SH-36 (super-high energy). Specimens 6-8 were tested non-instrumented.

Specimen id	F_{gy} (kN)	F_m (kN)	s_{gy} (mm)	s_m (mm)	s_t (mm)	W_{gy} (J)	W_m (J)	W_t (J)	KV (J)	KV/W_t	W_t-KV (J)
1	5.20	6.83	0.28	1.23	11.28	0.69	6.79	30.38	28.31	0.932	2.07
2	5.55	6.81	0.33	1.30	10.94	0.90	7.17	30.08	27.91	0.928	2.17
3	5.53	6.81	0.41	1.29	11.06	1.00	6.71	29.56	27.34	0.925	2.22
4	5.40	6.84	0.28	1.25	10.92	0.82	7.02	30.91	28.78	0.931	2.13
5	5.37	6.82	0.28	1.21	10.97	0.82	6.74	29.88	27.66	0.926	2.22
6									30.17		
7									30.05		
8									30.07		
N	5	5	5	5	5	5	5	5	8	5	5
Average	5.41	6.82	0.32	1.26	11.03	0.85	6.89	30.16	28.79	0.928	2.16
σ (abs)	0.141	0.013	0.057	0.038	0.148	0.114	0.200	0.514	1.166	0.003	0.064
CV	2.6%	0.2%	18.0%	3.1%	1.3%	13.5%	2.9%	1.7%	4.1%	0.3%	3.0%

With respect to the scatter of CVN test results documented in [17], the coefficients of variation for KV_{MCVN} are similar (KLST) or slightly higher (RHS[‡‡]): we obtained 2.5 % and 4.1 %, respectively, compared with CV = 2.5 % from CVN specimens. Values of absorbed energy W_t calculated from the instrumented test records provide slightly lower values of CV (1.6 % for KLST and 1.7 % for RHS) than for CVN tests (2.18 %). As far as force values are concerned, the scatter of CVN results from [17] (CV_{Fgy} = 1.3 % and CV_{Fm} = 0.4 %) is intermediate between the coefficients of variations calculated for KLST and RHS specimens.

We did not calculate sample sizes or perform outlier detection, given the limited number of super-high energy tests performed. These analyses will be done once additional MCVN test results are available.

[‡‡] Oddly enough, the three non-instrumented tests (see Table 11) yielded KV values greater than 30 J, clearly higher than those measured from the five instrumented tests, which ranged between 27.34 J and 28.31 J. The reason for this is unclear, but it obviously affects the value of the coefficient of variation (if non-instrumented test are ignored, we obtain CV = 2.0 %, *i.e.*, lower than for CVN specimens).

5. Additional aspects investigated

5.1 Comparison between different measures of absorbed energy (W_t and KV)

The result tables for all energy levels and MCVN specimen types also provide the ratio and the difference between instrumented total energy W_t and encoder absorbed energy KV for each instrumented test performed. Typically, the relationship between W_t and KV varies from machine to machine and depends on the characteristics of the instrumented striker, such as striker configuration (2 mm vs. 8 mm), position of strain gages, striker calibration, etc. [20,21].

At the high and super-high energy levels, the ratio KV/W_t is extremely consistent for both KLST and RHS tests, with coefficients of variations CV < 1 % (see Table 7 and Table 8 (high) and Table 10 and Table 11 (super-high)). At both energy levels, absolute values of KV/W_t are also similar for the two configurations (~0.9). At the low-energy level, more variability is observed, particularly for RHS specimens (CV = 3.6 %). For KLST specimens, CV is just above 1 % (1.3 %). Absolute values for KV/W_t are again relatively close for the two specimen types: 1.058 for KLST and 0.984 for RHS.

The average differences between KV and W_t are lower than 1 J at the low-energy level, less than 2 J at the high-energy level, and slightly higher than 2 J at the super-high energy level. Small differences between encoder and instrumented absorbed energies typically indicate a satisfactory performance of impact machine [20,21].

5.2 Correlation between full-size and miniaturized specimen absorbed energies

An extensive overview of the existing correlations of upper shelf energy (USE) data between full-size and miniaturized Charpy specimens was provided by Sokolov and Alexander [22]. An additional correlation approach was presented by the author [23].

The method commonly used in Europe consists of establishing an empirical ratio between full-size USE (USE_{fs}) and sub-size USE (USE_{ss}) based on a large number of tests. A different approach, often used by North American and Japanese researchers, correlates USE values with the ratio of various geometrical parameters, GP_x (with $x = fs$ or ss) for different specimen geometries in the form:

$$\frac{USE_{fs}}{USE_{ss}} = \frac{GP_{fs}}{GP_{ss}} \quad . \tag{2}$$

Eq. (2) can also be expressed in terms of a normalization factor NF, which is precisely the ratio of geometrical parameters mentioned above:

$$USE_{fs} = NF \times USE_{ss} \quad . \tag{3}$$

The most common expressions for NF that can be found in the literature are the following:

$$NF_1 = \frac{\left(Bb \right)_{fs}}{\left(Bb \right)_{ss}} \quad , \tag{4}$$

based on the ratio of fracture areas, with B = specimen thickness and b = ligament size [24,25];

$$NF_2 = \left[\frac{\beta b^{3/2} L}{\beta b^{3/2} L} \right]_{fs}$$ 　　，　　　　　　　　　　(5)

based on the ratio of nominal fracture volumes [24,25];

$$NF_3 = \frac{\left(\beta b^2 L \right)_{fs}}{\left(\beta b^2 L \right)_{ss}}$$ 　　，　　　　　　　　　(6)

based on a different expression for the ratio of nominal fracture volumes [26,27], and

$$NF_4 = \frac{\left(\dfrac{Bb^2}{LK_t} \right)_{fs}}{\left(\dfrac{Bb^2}{LK_t} \right)_{ss}}$$ 　　，　　　　　　　(7)

where L = span and K_t = elastic stress concentration factor [28].

In addition, Sokolov and Alexander [22] established empirical values NF_5 for 4 types of sub-size specimens considered in their study[§§] by averaging the values of USE_{fs}/USE_{ss} obtained on ten different materials (mostly pressure vessel steels with different heat treatments).

In [23], an exponential relationship between full-size and KLST values of USE was established, as shown in Figure 18. The best-fit regression curve relating USE_{fs} and USE_{KLST} is given by

$$USE_{fs} = 29.454 e^{0.2378 USE_{KLST}}$$ 　　．　　　　　　　　(8)
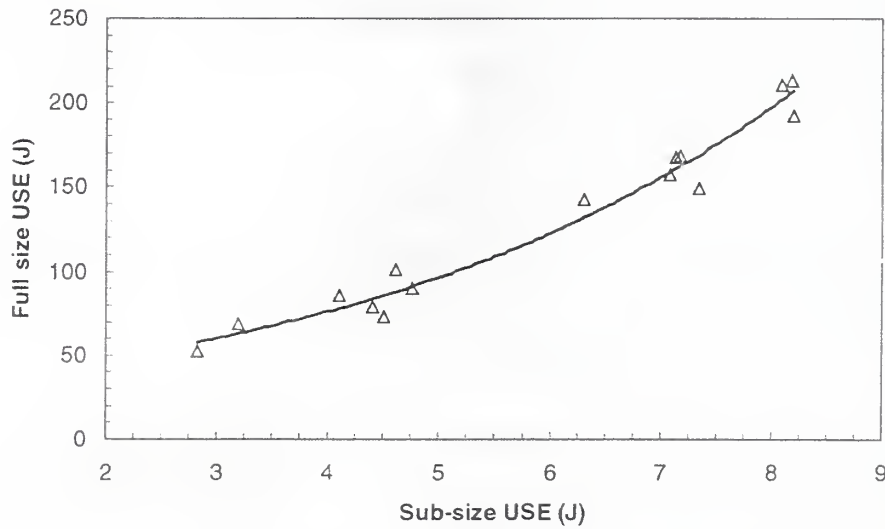
Figure 18 - Exponential correlation between sub-size and full-size USE values for KLST specimens [23].

[§§] In [22], sub-size specimen type 4 corresponds to KLST; sub-size specimen type 3 (cross section 5 mm × 5 mm, length 27 mm, span 20 mm) is dimensionally almost identical to RHS.

Finally, the average value of USE_{fs}/USE_{KLST} calculated in [23] for nine unirradiated and irradiated pressure vessel steels was $NF_7 = 21.6$.

A summary of the different normalization factors available for the miniaturized specimen geometries considered in this study (KLST and RHS), according to the methods listed above, is provided in Table 12.

Table 12 - Summary of normalization factors for estimating full-size *USE* based on miniaturized *USE*, see eq. (3). Note: the value of NF_6 [23] is not shown in the Table, because it depends on USE_{fs}.

Specimen type	NF_1 [Eq.(4)]	NF_2 [Eq.(5)]	NF_3 [Eq.(6)]	NF_4 [Eq.(7)]	NF_5 [22]	NF_7 [23]
KLST	8.9	26.5	23.7	13	24.9	21.6
RHS	4.3	8.9	8.9	2.8[***]	6.8[§§]	N/A

Considering the MCVN tests performed at three energy levels on KLST and RHS specimens, experimental normalization factors NF_{exp} were calculated by dividing the certified/average values of KV_{fs} at room temperature by the average MCVN absorbed energies for every data set. The results are shown in Table 13 and should be compared with the normalized factors listed in Table 12.

Table 13 - Experimental normalization factors obtained from NIST MVCN tests.

Energy level	Specimen type	$\overline{KV}$ (J)	$NF_{exp} = \dfrac{\overline{KV}_{fs}}{\overline{KV}_{ss}}$
Low	Full-size	18.2	-
	KLST	1.4	13.3
	RHS	3.4	5.3
High	Full-size	105.3	-
	KLST	5.2	20.2
	RHS	14.5	7.3
Super-high	Full-size	239.8	-
	KLST	9.7	24.8
	RHS	28.8	8.3

Theoretical (Table 12), empirical (Figure 18) and experimental (Table 13) normalization factors are compared in Figure 19 for KLST tests and in Figure 20 for RHS tests.

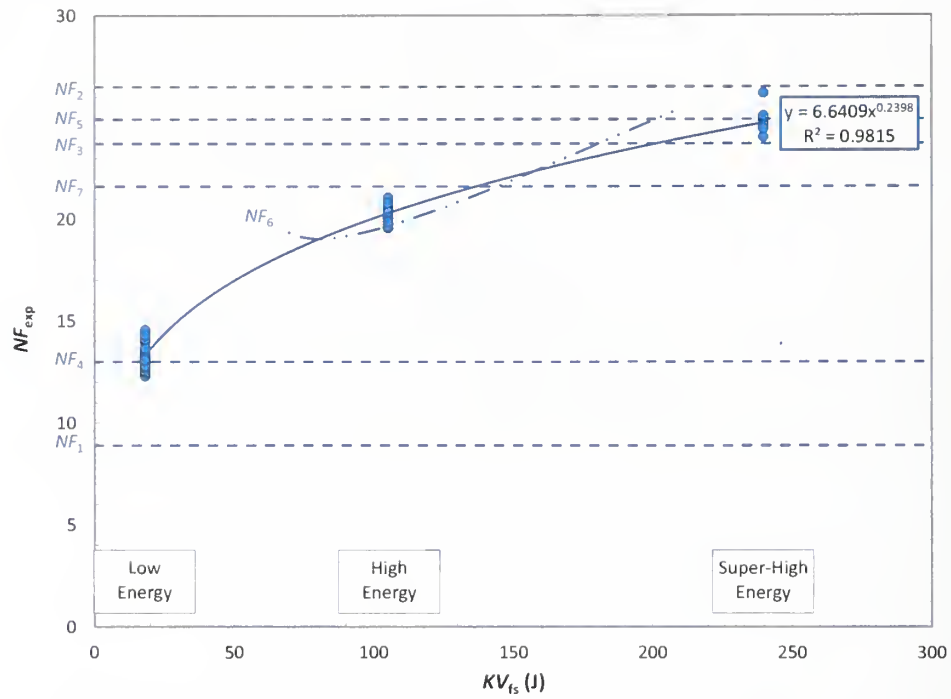[***] Values obtained for sub-size specimen type 3 (almost identical to RHS).

24

Figure 19 - Comparison between theoretical, empirical and experimental normalization factors for KLST specimens of different energy levels.
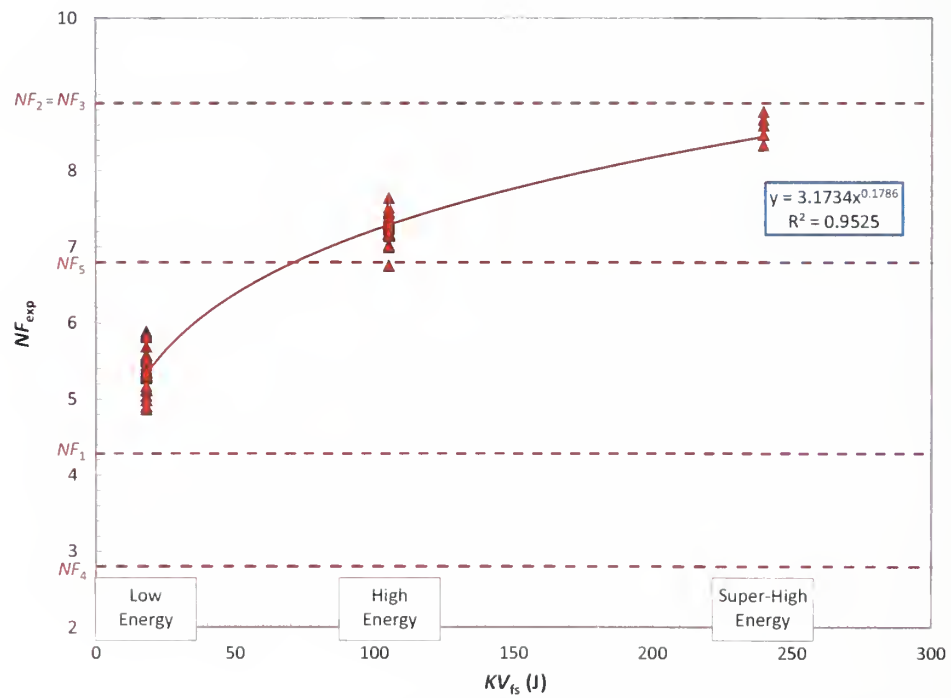

Figure 20 - Comparison between theoretical and experimental normalization factors for RHS specimens of different energy levels.

Another approach for evaluating the different normalization factors is shown in Figure 21 (KLST) and Figure 22 (RHS), where the certified or average values of KV_{fs} are compared with predictions obtained from KV_{ss} by the use of the various methods presented.

First of all, it must be stated that all the methods described above address *USE* values, rather than generic values of absorbed energy. At the high and super-high energy levels, analysis of the instrumented traces indicates fully ductile behavior; therefore it is legitimate to assume $KV = USE$. For low-energy specimens, however, the material's behavior is typical of the ductile-to-brittle transition regime (shear fracture appearance values, estimated through the analysis of the instrumented test record, ranged between 40 % and 60 % for KLST specimens and between 30 % and 50 % for RHS specimens).

The most immediate conclusion emerging from Figure 19 and Figure 20 is that normalization factors are not independent of absorbed energy. Furthermore, full-size KV values estimated by means of normalization factors NF_1 and NF_4 are acceptable only at the low energy level, while at higher energies they are severely underpredicted. Conversely, non-conservative estimations were generally obtained through the use of NF_2. Mixed results are observed for NF_3, NF_5 and NF_6. Equation (8) works only for KLST tests at the high-energy level, *i.e.*, when both KV_{fs} and KV_{KLST} are within the ranges for which the relationship was developed (Figure 18). In short, none of the approaches considered appears convincing for all energy levels and both MCVN miniaturized specimen types.
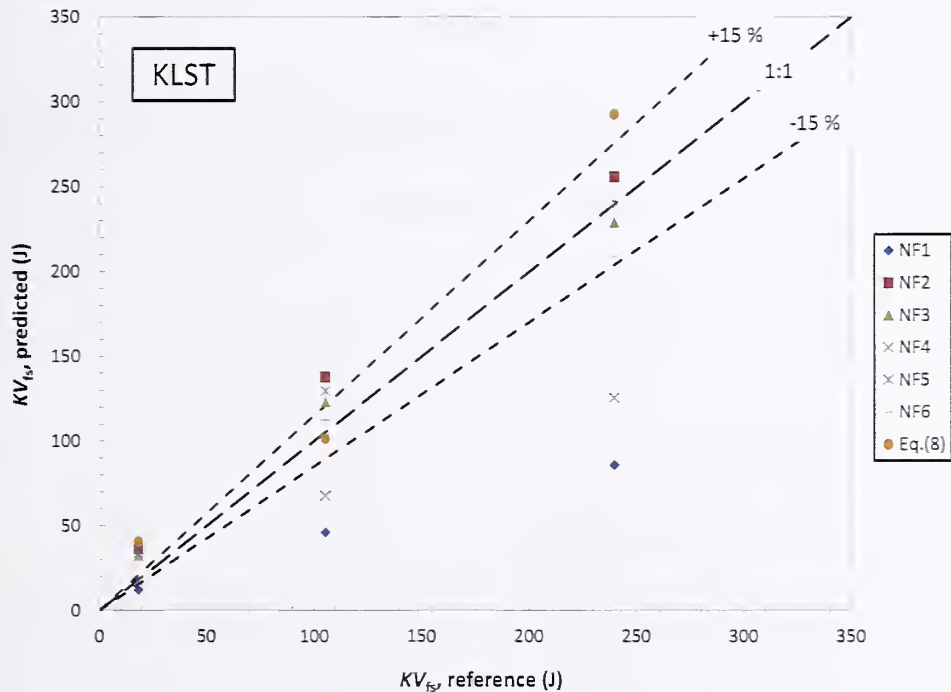

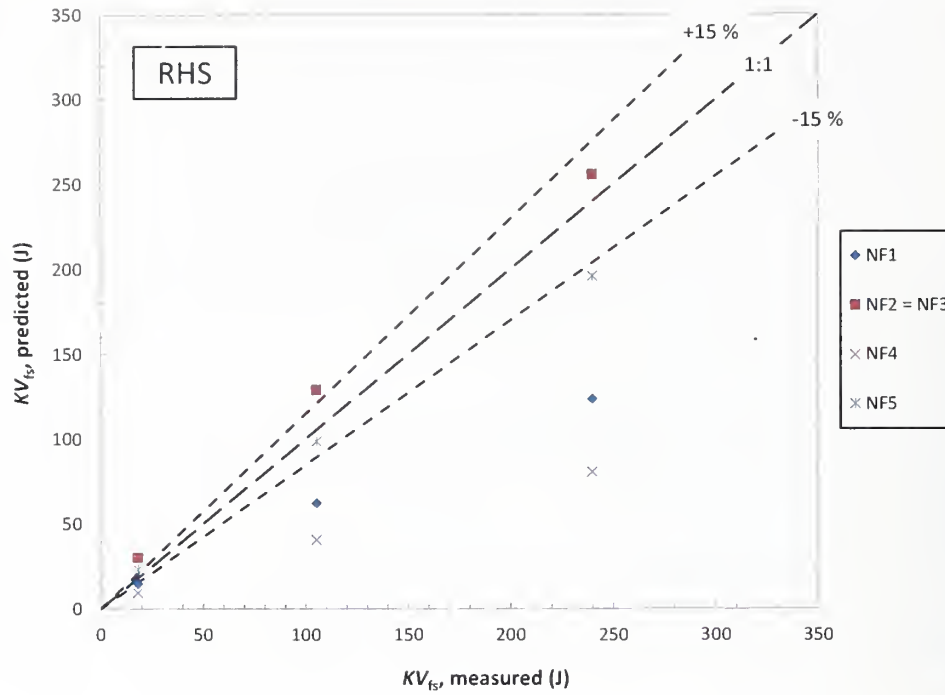Figure 21 - Prediction of full-size absorbed energy from KLST specimens by use of different approaches.

Figure 22 - Prediction of full-size absorbed energy from RHS specimens with different approaches.

Based on our test results, the following relationships between KV_{ss} and KV_{fs} were obtained:

$$KV_{fs} = 12.102 \cdot KV_{KLST}^{1.313} \tag{9}$$

for KLST specimens (with coefficient of determination $R^2 = 0.9981$), and

$$KV_{fs} = 4.1397 \cdot KV_{RHS}^{1.2091} \tag{10}$$

for RHS specimens (with $R^2 = 0.9978$).

5.3   Symmetrical versus asymmetrical fracture

When a Charpy specimen fractures, shear lips are formed unless the material is fully brittle (*i.e.*, shear fracture appearance = 0 %). Shear lips are jagged edges generated at the lateral borders of the fracture surface. Their magnitude (height) is directly related to amount of ductility exhibited by the Charpy specimen at the test temperature. When shear lips are visible on a tested Charpy specimen, the fracture is defined symmetrical if both shear lips are on the same specimen half, and asymmetrical if each specimen half exhibits one shear lip (Figure 23).
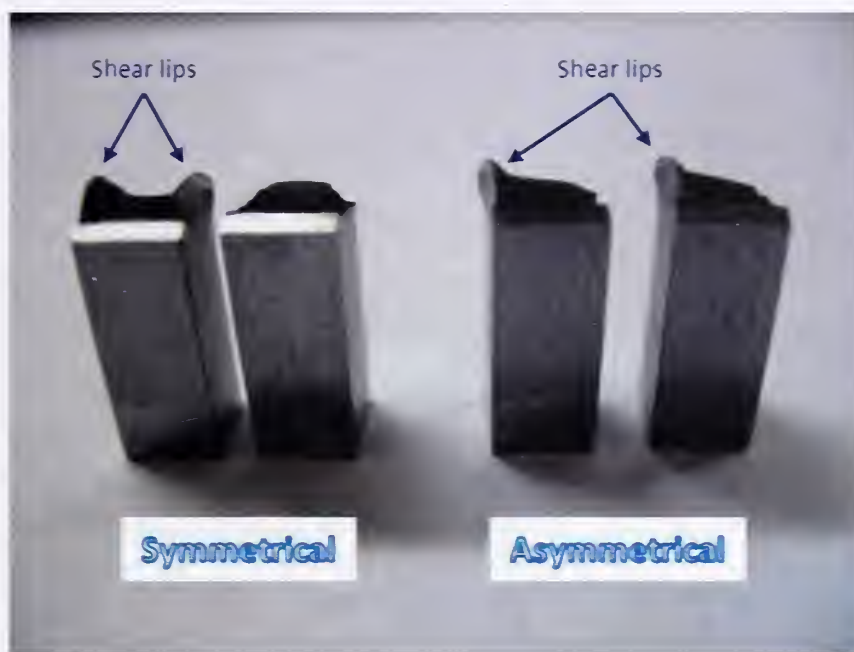
Figure 23 – Examples of symmetrical and asymmetrical fracture on high-energy RHS specimens.

Earlier investigations at NIST [29,30] conducted on full-size verification specimens of high and super-high energy showed that the symmetry of shear lip formation has a significant influence on absorbed energy. Specifically, asymmetrical fractures are generally associated with higher absorbed energies.

For the MCVN specimens tested at NIST for this study, the information on fracture symmetry is summarized in Table 14.

Table 14 - Symmetrical (S) and asymmetrical (A) fractures for MCVN tests performed at NIST.

Energy level	Specimen type	Type of fracture	No. of tests	$\overline{KV}$ (J)	σ_{KV} (J)
Low	KLST	S	18 (56 %)	1.37	0.046
		A	14 (44 %)	1.36	0.078
	RHS	S	16 (50 %)	3.47	0.127
		A	16 (50 %)	3.38	0.198
High	KLST	S	12 (38 %)	5.12	0.062
		A	20 (63 %)	5.25	0.091
	RHS	S	14 (44 %)	14.28	0.239
		A	18 (56 %)	14.67	0.373
Super-High	KLST	S	6 (75 %)	9.58	0.217
		A	2 (25 %)	9.90	0.120
	RHS	S	8 (100 %)	28.79	1.166
		A	0 (0 %)	-	-

The likelihood of symmetrical or asymmetrical fracture appears close at low and high energies, while at the super-high energy level, symmetrical fracture clearly prevails. In order to statistically assess the influence of fracture symmetry on absorbed energy, Student's t-test [31] was applied to the means of KV for specimens fracturing symmetrically and asymmetrically for each MCVN configuration and nominal energy level.

The specific *t*-test used is the unpaired two-sample location test, which verifies the null hypothesis that the means of two normally distributed populations are equal. The results obtained are summarized in Table 15.

Table 15 – Results of Student's *t*-test for MCVN tests performed at NIST.

Energy level	Specimen type	Type of fracture	$\overline{KV}$ (J)	Two-tailed *P* value	*t*	Standard error of difference	Test result
Low	KLST	S	1.37	0.8327	0.2080	0.023	Means are <u>not</u> statistically different
		A	1.36				
	RHS	S	3.47	0.1213	1.5945	0.059	Means are <u>not</u> statistically different
		A	3.38				
High	KLST	S	5.12	0.0001	4.4804	0.030	Means are statistically <u>extremely</u> different
		A	5.25				
	RHS	S	14.28	0.0022	3.3579	0.116	Means are statistically <u>very</u> different
		A	14.67				
Super-High	KLST	S	9.58	0.1050	1.9078	0.167	Means are <u>not</u> statistically different
		A	9.90				
	RHS	S	28.79	-	-	-	-
		A	-				

NOTE – The *P* value can be interpreted as the probability of the difference between sample means being coincidental.

The results of the statistical analyses show that fracture symmetry has no significant influence at low-energy level, whereas at high-energy level, asymmetric fracture is associated with higher absorbed energies. Results at super-high level (only KLST specimens) are not reliable due to the limited sample sizes (only twoasymmetrical fractures). These results are consistent with the findings reported in [29,30], where only high and super-high verification specimens were analyzed.

5.4 Broken versus unbroken specimens

Another characteristic feature of Charpy testing is the fact that, after being struck by the hammer, specimens may exit the anvils either broken in two pieces or unbroken. The latter happens when the material is ductile enough to be bent and pushed out through the anvils by the striker before being fully fractured. In some cases, tested specimens are still in one piece, but the remaining ligament is so thin that samples can be easily broken by applying moderate force with one's fingers. In this case, the specimen is classified as "finger broken," and for practical purposes is considered equivalent to "broken."[†††] Note also that, according to ASTM E23-07[ε1], for unbroken specimens, the percent shear fracture is conventionally given as 100 %.

Chandavale and Dutta [32] investigated the amount of impact energy spent for tossing the specimen. This toss energy is considered an error in the absorbed energy value returned by the machine encoder, which should be subtracted from *KV* in order to obtain the real fracture energy. A combination of theoretical calculations and experiments showed that, for a low-carbon steel (ASTM A516 Gr. 70) tested at room temperature on a 300-J pendulum and providing $KV \approx 100$ J, this error is on the order of 1.25 J. IF the average ratio between CVN and

---

[†††] Section 9.2.2 of ASTM E23-07[ε1] reads: "The lateral expansion of an unbroken specimen can be reported as broken if the specimen can be separated by pushing the hinged halves together once and then pulling them apart without further fatiguing the specimen (…)".

MCVN absorbed energies calculated from high-energy NIST tests (see section 5.2) is used, this error would correspond to 0.06 J for KLST and 0.17 J for RHS.

In the case of miniaturized Charpy specimens, the reduced dimensions enhance material ductility and thus increase the likelihood of specimens exiting the pendulum unbroken. This is particularly true for KLST specimens, which are more slender than RHS and have a larger span value (22 mm instead of 19.3 mm).

The information concerning the percentage of broken and unbroken MCVN specimens from NIST tests is provided in Table 16.

Table 16 - Percentages of broken (B), finger-broken (FB) and unbroken (U) specimens for the MCVN tests performed at NIST.

Energy level	Specimen type	No. of tests	B	FB	U
Low	KLST	32	32 (100 %)	0 (0 %)	0 (0 %)
	RHS	32	32 (100 %)	0 (0 %)	0 (0 %)
High	KLST	32	0 (0 %)	14 (44 %)	18 (56 %)
	RHS	32	7 (22 %)	19 (59 %)	6 (19 %)
Super-High	KLST	8	0 (0 %)	0 (0 %)	8 (100 %)
	RHS	8	0 (0 %)	0 (0 %)	8 (100 %)

At the low and super-high energy level, all MCVN specimens tested exit the anvils broken or unbroken, respectively. For high-energy specimens, however, constraint conditions can vary from specimen to specimen, and specimens can be broken, finger-broken or unbroken. At this energy level, a clear difference can be observed between KLST and RHS, with the former specimen type providing clearly more unbroken tests (56 %) than the latter (19 %). Moreover, none of the tested KLST specimen exited the anvils in two pieces (*i.e.*, B = 0 %). As previously mentioned, different specimen proportions and anvil spacing are the causes for these differences in behavior.

For high-energy KLST specimens, an unpaired two-tailed t-test detected a statistically extremely significant difference (P-value < 0.0001) between the mean KV of finger-broken (5.12 J) and unbroken (5.26 J) specimens. Note also that all the unbroken specimens exhibited asymmetrical fracture, while the percentage of symmetrical and asymmetrical fractures among the finger-broken specimens was 86 % and 14 %, respectively. In the case of RHS specimens, the t-test failed to detect a clear statistical significant difference (P-value = 0.0610) between the mean KV of broken/finger-broken (14.44 J) and unbroken (14.78 J) specimens[‡‡‡]. For broken/finger-broken RHS specimens, fractures are nearly equally split between symmetrical (54 %) and asymmetrical (46 %); all six unbroken specimens exhibited asymmetrical fracture.

[‡‡‡] This is probably due to the small sample size of the unbroken specimens (6 %).

6. Conclusions

This report describes the experimental results obtained at NIST by testing miniaturized Charpy specimens of two different configurations (KLST and RHS) at three energy levels (low, high and super-high). These tests constitute the preliminary qualification phase of a NIST project aimed at producing a new SRM, *i.e.*, miniaturized reference specimens for the indirect verification of small-scale impact testing machines.

The most important conclusions for the NIST project are the following:

1. The new small-scale instrumented impact tester purchased by NIST was successfully qualified by testing KLST specimens of the JRQ pressure vessel steel and comparing the results with data from an international Round-Robin conducted by a European technical committee in the mid-90s. Excellent agreement between NIST and Round-Robin data was observed.

2. The results obtained for absorbed energy KV from MCVN specimens at low and high energy indicate that production and certification of a new SRM may be feasible for the verification of both absorbed energy and maximum force. Coefficients of variation and sample sizes for MCVN specimens were slightly higher than for full-size specimens at low energy, and very similar at high energy. In general, result variability was smaller for KLST than for RHS. For maximum forces, the coefficients of variations from NIST tests, which range from 0.6 % to 1.8 %, are smaller than those reported for the Round-Robin that qualified the dynamic force verification specimens from the same batches (2.3 % for low energy and 1.2 % for high energy). Outlier analysis was performed with box-and-whiskers plots and Grubbs' tests. For both low-energy and high-energy tests, outlier values were detected by Grubbs' test for forces at general yield. One RHS high-energy specimen was also classified as an outlier by the box-and-whiskers method but not by Grubbs' test at the $\alpha = 0.01$ significance level.

3. At the super-high energy level, a limited number of MCVN specimens (eight) were tested. The aim of these tests was to determine whether absorbed energy values would differ significantly from those obtained at the high-energy level. The answer is clearly affirmative: for KLST and RHS specimens, we obtained average values $KV = 9.66$ J and 28.79 J, respectively. For comparison, average KLST and RHS values at the high-energy level were $KV = 5.20$ J and 14.49 J. This justifies the continued development of super-high energy MCVN verification specimens. Additional tests on super-high energy MCVN specimens will be performed in the continuation of this project.

Additional research aspects were also investigated in this preliminary phase of the project. The most significant conclusions are summarized here:

(a) For the NIST instrumented small-scale impact tester, the relationship between absorbed energies returned by the encoder (KV) and calculated from the test record (W_t) is quite consistent. The ratio $KV/W_t \approx 1.0$ at low energy and $KV/W_t \approx 0.9$ at high and super-high energy. The performance of the machine can be considered satisfactory.

(b) Average energy values from MCVN specimens were correlated to certified/average energy values for full-size specimens at the corresponding energy levels. The results were compared to normalization approaches published in the literature. It is clear that normalization factors (KV_{CVN}/KV_{MCVN}) are not constant, but depend on the energy level and possibly also material's strength. It was found that none of the published methods was

31

fully satisfactory at all energy levels. Empirical correlations were obtained for KLST and RHS specimens by fitting the data with power-law curves.

(c) We investigated the relationship between fracture symmetry (*i.e.*, both shear lips on the same specimen half or one on either half) and absorbed energy, as well as the relative frequency of symmetrical and asymmetrical fracture at the different energy level. At low energies, both types of fracture appear equally likely, but no influence was detected on absorbed energy by use of statistical tools (Student's *t*-test). At high and super-high energies, asymmetrical fracture is more likely to occur and was found to be associated with higher absorbed energies. This is consistent with a previous study conducted at NIST on full-size verification specimens.

(d) Another feature we looked at is whether specimens are fully broken, "finger-broken" or unbroken after being tested. At low and super-high energy levels, respectively, all specimens exit the anvils fully broken and unbroken. For the high-energy specimens, a mix of broken/finger broken and unbroken specimens was observed, with KLST specimens showing a more pronounced tendency to exit the anvils unbroken. Unbroken samples are also associated with a statistically higher absorbed energy.

In the next phase of this project, it is planned to organize an international Round-Robin on MCVN testing that will involve highly qualified and experienced laboratories in the U.S. and overseas. Results will be analyzed in accordance with ASTM E691-11 [11] in order to establish certified values of absorbed energy and maximum force at low, high, and super-high energy levels.

Acknowledgements

Bibliography

[1] D. E. Driscoll, "Reproducibility of Charpy Impact Test, " in *Symposium on Impact Testing*, ASTM STP 176, F. G. Tatnall, ed., American Society for Testing and Materials, Philadelphia, PA, 1955, pp. 70-75.

[2] T. A. Siewert, M. P. Manahan, C. N. McCowan, J. M. Holt, F. J. Marsh, and E. A. Ruth, "The History and Importance of Impact Testing, " in *Pendulum Impact Testing: A Century of Progress*, ASTM STP 1380, T. A. Siewert and M. P. Manahan, Sr., Eds., American Society for Testing and Materials, West Conshohocken, PA, 1999, pp. 3-16.

[3] C. N. McCowan, T. A. Siewert, and D. P. Vigliotti, "Charpy Verification Program: Reports Covering 1989-2002," NIST Technical Note 1500-9, September 2003.

[4] E. Lucon, R. Chaouadi, A. Fabry, J.-L. Puzzolante, and E. van Walle, "Characterization of materials properties by use of full size and subsize Charpy tests: an overview of different correlation procedures," in *Pendulum Impact Testing: A Century of Progress*, ASTM STP 1380, T.A. Siewert, Ed., ASTM, Philadelphia, PA, 2000, pp. 146-163.

[5] ISO 14556:2000, "Steel -- Charpy V-notch pendulum impact test -- Instrumented test method," International Organization for Standardization, www.iso.org.

[6] M. P. Manahan and C. Charles, "A Generalized Methodology for Obtaining Quantitative Charpy Data From Test Specimens of Nonstandard Dimensions," *Nuclear Technology*, Vol. 90, 1990, pp. 245-259.

[7] ASTM E2248-09, "Standard Test Method for Impact Testing of Miniaturized Charpy V-Notch Specimens," ASTM Book of Standards, Vol. 03.01.

[8] Home page of the Generation IV International Forum, http://www.gen-4.org/.

[9] IFMIF home page, http://www.frascati.enea.it/ifmif/.

[10] M. P. Manahan, F. J. Martin, and R. B. Stonesifer, "Results of the ASTM Instrumented/Miniaturized Round Robin Test Program", in *Pendulum Impact Testing: A Century of Progress*, ASTM STP 1380, T. A. Siewert and M. P. Manahan, Sr., Eds., American Society for Testing and Materials, West Conshohocken, PA, 1999, pp. 223-241.

[11] ASTM E691-11, "Standard Practice for Conducting an Interlaboratory Study to Determine the Precision of a Test Method," ASTM Book of Standards, Vol. 14.02.

[12] E. Lucon, G. Roebben, J.-L. Puzzolante, and A. Lamberty, "Impact Characterization of Sub-Size Charpy V-Notch Specimens Prepared from Full-Size Certified Reference Charpy V-Notch Test Pieces," *Journal of ASTM International*, Vol. 2, No. 7, 2005.

[13] E. Lucon, "European activity on instrumented impact testing of subsize Charpy V-notch specimens (ESIS TC5)," in *Pendulum Impact Testing: A Century of Progress*, ASTM STP 1380, T. A. Siewert and M. P. Manahan, Sr., Eds., American Society for Testing and Materials, West Conshohocken, PA, 1999, pp. 242-252.

[14] "Reference manual on the IAEA JRQ correlation monitor steel for irradiation damage studies," IAEA-TECDOC-1230, International Atomic Energy Authority, Vienna (Austria) July 2001.

[15] ASTM E2298-09, "Standard Test Method for Instrumented Impact Testing of Metallic Materials," ASTM Book of Standards, Vol. 03.01.

[16] C. N. McCowan, J. D. Splett, and E. Lucon, "Dynamic Force Measurement: Instrumented Charpy Impact Testing," NISTIR 6652, National Institute of Standards and Technology, January 2008.

[17] C. N. McCowan, E. Lucon, and R. L. Santoyo, "Evaluation of Bias for Two Charpy Impact Machines with the Same Instrumented Striker," *Journal of ASTM International*, Vol. 8, No. 5, 2011.

[18] C. N. McCowan, T. A. Siewert, and D. P. Vigliotti, "The NIST Charpy V-notch Verification Program: Overview and Operating Procedures," in *Charpy Verification Program: Reports Covering 1989-2002*, NIST Technical Note 1500-9, September 2003.

[19] F. Grubbs, "Procedures for Detecting Outlying Observations in Samples," *Technometrics*, 11(1), 1969, pp. 1-21.

[20] E. Lucon, R. Chaouadi, and E. van Walle, "Different Approaches for the Verification of Force Values Measured with Instrumented Charpy Strikers," in *Pendulum Impact Machines: Procedures and Specimens,*

ASTM STP 1476 (Eds: T. Siewert, M. Manahan, and C. McCowan), ASTM, West Conshohocken, PA, 2006, pp. 95-102.

[21] E. Lucon, "On the Effectiveness of the Dynamic Force Adjustment for Reducing the Scatter of Instrumented Charpy Results," *Journal of ASTM International*, Vol. 6, No. 1 (January 2009).

[22] M. A. Sokolov and D. J. Alexander, "An Improved Correlation Procedure for Subsize and Full-Size Charpy Impact Specimen Data, " NUREG/CR-6379, ORNL-6888, March 1997.

[23] E. Lucon, R. Chaouadi, A. Fabry, J.-L. Puzzolante, and E. van Walle, "Characterisation of materials properties by use of full size and subsize Charpy tests: an overview of different correlation procedures," in Pendulum Impact Testing: A Century of Progress, ASTM STP 1380 (Ed: T.A. Siewert), ASTM, Philadelphia, PA 2000, pp. 146-163.

[24] W. R. Corwin, R. L. Klueh, and J. M. Vitek, "Effect of specimen size and nickel content on the impact properties of 12 Cr-1 MoVW ferritic steel," *Journal of Nuclear Materials* Vol. 122, Issues 1-3, 1984, pp. 343-348.

[25] W. R. Corwin, and A. M. Hougland, "Effect of Specimen Size and Material Condition on the Charpy Impact Properties of 9Cr-1Mo-V-Nb Steel," in *The Use of Small-Scale Specimens for Testing Irradiated Material*, ASTM STP 888 (Eds: W. R. Corwin, G. E. Lucas), ASTM, Philadelphia, PA 1986, pp. 325-338.

[26] G. E. Lucas, G. R. Odette, J. W. Sheckherd, P. McConnell, and J. Perrin, "Subsized Bend and Charpy V-Notch Specimens for Irradiated Testing," in *The Use of Small-Scale Specimens for Testing Irradiated Material*, ASTM STP 888 (Eds: W. R. Corwin, G. E. Lucas), ASTM, Philadelphia, PA 1986, pp. 304-324.

[27] G. E. Lucas, G. R. Odette, J. W. Sheckherd, and M. R. Krishnadev, "Recent Progress in Subsized Charpy Impact Specimen Testing for Fusion Reactor Materials Development," *Fusion Technology* Vol. 10, 1986, pp. 728-733.

[28] B. S. Louden, A. S. Kumar, F. A. Garner, M. L. Hamilton, and W. L. Hu, "The influence of specimen size on charpy impact testing of unirradiated HT-9," *Journal of Nuclear Materials* Vol. 155-157, 1988, pp. 662-667.

[29] C. N. McCowan, J. Pauwels, G. Revise, and H. Nakano, "International Comparison of Impact Verification Programs," in *Pendulum Impact Testing: A Century of Progress*, ASTM STP 1380, T.A. Siewert, ed., ASTM, Philadelphia, PA, 2000, pp. 73-89.

[30] C. N. McCowan and D. P. Vigliotti, "The Influence of Shear Lip Symmetry on the Absorbed Energy of Charpy Impact Specimens," in *Charpy Verification Program: Reports Covering 1989-2002*, NIST Technical Note 1500-9, September 2003.

[31] Student (*pseudonym of W. S. Gossett*), "The Probable Error of a Mean," *Biometrika* (1908), Vol. 6(1), pp. 1-25.

[32] R. G. Chandavale and T. Dutta, "Correction of Charpy Impact Values for Kinetic Energy of Test Specimens," in *Pendulum Impact Machines: Procedures and Specimens for Verification*, ASTM STP 1248, T.A. Siewert and A. K. Schmieder, eds., ASTM, Philadelphia, PA, 1995, pp. 221-231.